Thinning of articular cartilage after joint unloading or immobilization. An experimental investigation of the pathogenesis in mice

Nomura, Masato ; Sakitani, Naoyoshi ; Iwasawa, Hiroyuki ; Kohara, Yuta ; Takano, Shoko ; Wakimoto, Yoshio ; Kuroki, Hiroshi ; Moriyama, Hideki

(Citation)
Osteoarthritis and Cartilage,25(5):727-736

(Issue Date)
2017-05

(Resource Type)
journal article

(Version)
Accepted Manuscript

(URL)
https://hdl.handle.net/20.500.14094/90004510

Thinning of articular cartilage after joint unloading or immobilization. An experimental investigation of the pathogenesis in mice

Masato Nomura, M.Sc., Naoyoshi Sakitani, M.Sc., Hiroyuki Iwasawa, M.Sc., Yuta Kohara, B.Sc., Shoko Takano, B.Sc., Yoshio Wakimoto, M.Sc., Hiroshi Kuroki, Ph.D., Hideki Moriyama, Ph.D.

M. Nomura (cunorimousiraty@gmail.com)

N. Sakitani (7asdfghjklzxcvbnm@gmail.com)

Y. Kohara (kohakoha1313@gmail.com)

S. Takano (shoko.12.t@gmail.com)

Y. Wakimoto (wakio0820.kbu@gmail.com)

H. Moriyama (morihide@harbor.kobe-u.ac.jp)

Department of Rehabilitation Science, Graduate School of Health Sciences, Kobe University., Tomogaoka 7-10-2, Suma-ku, Kobe 654-0142, Japan.

H. Iwasawa (googrie588@gmail.com)

Department of Rehabilitation, St. Marianna University School of Medicine., Sugao 2-16-1, Miyamae-ku, Kawasaki 216-8511, Japan

Department of Rehabilitation Science, Graduate School of Health Sciences, Kobe University.,
Tomogaoka 7-10-2, Suma-ku, Kobe 654-0142, Japan.

H. Kuroki (kuroki.hiroshi.6s@kyoto-u.ac.jp)
School of Health Sciences, Graduate School of Medicine, Kyoto University., Kawahara-cho,
Shogoin 53, Sakyo-ku, Kyoto-shi, Kyoto 606-8507, Japan.

Corresponding author:
Hideki Moriyama, Ph.D.
Professor
Department of Rehabilitation Science, Graduate School of Health Sciences, Kobe University
Tomogaoka 7-10-2, Suma-ku, Kobe 654-0142, Japan.
Tel & Fax +81 78 796 4574
E-mail morihide@harbor.kobe-u.ac.jp

Running title: Cartilage degeneration by disuse

Abstract

Objective: Moderate mechanical stress generated by normal joint loading and movement is essential for the maintenance of healthy articular cartilage. However, the effects of reduced loading caused by the absence of weight bearing or joint motion on articular cartilage and subchondral bone is still poorly understood. We aimed to characterize morphological and metabolic responses of articular cartilage and subchondral bone to decreased mechanical stress in vivo.

Methods: Mice were subjected to periods of hindlimb unloading by tail suspension or external fixation of the knee joints. The articular surface was observed with digital microscope and the epiphyseal bone was assessed by micro-CT analysis. Articular cartilage and subchondral bone were further evaluated by histomorphometric, histochemical, and immunohistochemical analyses.

Results: The joint surface was intact, but thickness of both the total and uncalcified layer of articular cartilage were decreased both after joint unloading and immobilization. Subchondral bone atrophy with concomitant marrow expansion predisposed osteoclast activity at bone surface to invade into cartilaginous layer. Uncalcified cartilage showed decreased aggrecan content and increased aggrecanase expression. Alkaline phosphatase activity was increased at uncalcified cartilage, whereas decreased at calcified cartilage. The distributions of hypertrophic chondrocyte markers remained unchanged.

Conclusion: Thinning of articular cartilage induced by mechanical unloading may be mediated by metabolic changes in chondrocytes, including accelerated aggrecan catabolism and exquisitely modulated matrix mineralization, and cartilage matrix degradation and resorption by subchondral osteoclasts. Cartilage degeneration without chondrocyte hypertrophy under unloading condition indicate the possible existence of mechanism which is different from osteoarthritis pathogenesis.

Key words: Mechanical unloading, Articular cartilage, Aggrecan, Mineralization, Subchondral bone, Osteoclast

Introduction

Moderate mechanical stress generated by normal joint loading and movement is essential for the maintenance of healthy articular cartilage. Although cartilage within a physiological range of mechanical stress assures the optimal balance between anabolic and catabolic phenomena[1], overloading induces catabolic chondrocyte responses[2] and is well known to be one of the main causes of osteoarthritis (OA)[3]. In addition, the reduction of applied load (caused by joint disuse) has also been reported to be harmful to articular cartilage[4].

Animal models of joint unloading or immobilization have been used extensively to study the effects of decreased mechanical stress on joint structures, including articular cartilage. Numerous animal studies demonstrated that joint immobilization by casting or surgery induces changes in cartilage thickness[5-15], number of chondrocytes[8-17], extracellular matrix components[7,9-25], and cartilage surface irregularity or fibrillation[11-17,25-27]. These alterations were often associated with contracture development. However, most of these animal studies on joint immobilization observed articular cartilage mainly at the contact areas in fixed position, and several authors including Langenskiöld *et al.*[25] attributed this cartilage degradation by loss of joint motion to compression necrosis, rather than reduced loading.

Only 5 prior studies attempted to assess the influence of joint unloading without motion restriction on the articular cartilage, using animal models of ipsilateral paw transection[29] or tail suspension[5,30-32]. In these studies, unloading led to increased or decreased or unchanged thickness of cartilage[5,29,31,32], decreased or unchanged number of chondrocytes[29,30,32], existence or non-existence of chondrocyte hypertrophy and cluster[29,31,32], reduced proteoglycan content[29,31,32], tidemark advancement[5,31], and existence or non-existence of subchondral vascular encroachment into the cartilage[5,31].

There has been a growing interest in the effect of reduced loading on articular cartilage, since a recent study on patients with ankle fracture reported that 7 weeks of partial load bearing led to decrease in knee cartilage thickness, volume, and surface area[33]. However, in earlier animal studies[5,29-32], there is no consensus about morphological changes of articular cartilage after unloading. In addition, chondrocyte differentiation, survival, and metabolic characteristics in the pathogenesis is still poorly investigated, and cross-talk between subchondral bone and articular cartilage under unloading condition remains unclear. Despite the clinical importance of cartilage degeneration by disuse such as during prolonged bed rest or long-term space flight, exercise is the only effective safeguard conceivable, as its pathology remain elusive.

The goal of this study was to gain a comprehensive picture of pathology in cartilage alteration by mechanical unloading. We applied hindlimb unloading by tail suspension or surgical immobilization of the knee joints in mice. Entire knee joints are exposed to unloading in tail suspended mice, while non-contact regions in immobilized mice. We examined morphological responses of articular cartilage and subchondral bone after mechanical unloading, and sought to determine possible pathological factors contributing to the morphological changes.

Method

Experimental animals and animal care

Thirty male C57BL/6J mice of 7 weeks of age were purchased from Japan SLC (Shizuoka, Japan). Acclimated for 1 week, randomly selected six mice were killed and served as control, while the remaining 24 mice were equally divided into two experimental groups: hindlimb unloaded (HU) and immobilized (IM). The animals in each experimental group were assigned to 3 subgroups (n = 4 per group), corresponding to the time of examination after unweighting or immobilization: 2, 4, and 8 weeks.

For the HU group, animals underwent tail suspension with a modified unloading method based on the traditional NASA Morey-Holton design[34]. Briefly, mice were anesthetized by intraperitoneal administration of 40 mg/kg sodium pentobarbital and subcutaneously injected with 0.02 mg/kg buprenorphine to give relief of pain. A sterile steel wire was inserted into an intervertebral space of the tail and the steel wire was shaped into a ring for later suspension. Connecting the tail ring by string to track hanged from the ceiling, we enabled the animals to roam freely throughout the entire cage. The head down tilt angle was monitored every day throughout the experimental period and remained at approximately 30° [Supplementary Fig. 1(A)], so that 50% of the body weight was distributed to the forelimbs[35].

The right and left knees of each animal in the IM group were surgically immobilized according to the modified method described by Nagai *et al*.[36]. In brief, a longitudinal incision was made through the lateral skin of the femur and the tibia under anesthesia. 2 cm-long kirschner wires of 0.6 mm in diameter were then screwed into the both diaphysises. After the skin were closed with silk suture, the two kirschner wires were externally fixed with wire and resin to maintain knee flexion of approximately 140 ± 5° [Supplementary Fig. 1(B)]. Postoperatively, the animals had appropriate pain control by subcutaneous dose of 0.02 mg/kg buprenorphine once daily for 5 days. We confirmed in a pilot study that kirschner

wires penetrated through bones and no fracture occurred by micro-computed tomography (μCT) scanning [Supplementary Fig. 1(C)] and that rigid immobilization was maintained for more than 8 weeks after surgery.

The right and left knees served as different samples. They were housed in plastic cages in a room with controlled environmental conditions, and had free access to water and standard food. This study was approved by the Institutional Animal Care and Use Committee and carried out according to the Kobe University Animal Experimentation Regulation.

Microscopic and Scanning Electron Microscopic (SEM) Observation

At the end of the experimental period, the half of the animals in each group were euthanized by exsanguination under anesthesia. Knee joints were removed by dissection and disarticulated. Entire articular surface of the femoral condyle and tibial plateau were imaged using digital microscope (VHX-5000; Keyence, Osaka, Japan) and high-resolution zoom lens (VH-ZST; Keyence) under x 200 magnification. SEM images were subsequently obtained at the magnification of x 2000 with free-angle observation system (VHX-D510; Keyence).

μCT Analysis

159

160 After the observations of cartilage surface, the samples of distal femur and proximal
161 tibia were scanned separately by micro 3D x-ray CT system (R_mCT2; Rigaku, Tokyo,
162 Japan) with an isotropic voxel resolution of 10 μm (x-ray tube potential = 90 kV, current =
163 160 μA, and a scan time of 3 min per sample). 3D images were reconstructed and were
164 analyzed with TRI/3D-BON software (Ratoc, Tokyo, Japan). Bone volume density (bone
165 volume/total volume; BV/TV) were measured on the epiphyseal regions.

166

167 *Histology*

168

169 *Histological preparation*

170

171 Undecalcified frozen sections were prepared according to the method described by
172 Kawamoto[37]. Briefly, the whole knee joints including the patella and joint capsule were
173 harvested from the animals of half the number in each group. Knee samples were then freeze-
174 embedded with 5% carboxymethyl cellulose gel at the angle of maximum flexion
175 (approximately 140 ± 5°; equal to that of immobilized). Blocks were cut into slices from
176 medial side of the knees, and 5-μm sagittal sections were prepared at the level which is 50-
177 200 μm lateral from the level that the medial meniscus separates into anterior and posterior

horns.

Determination of Regions for Assessment

We originally determined the cartilage regions for assessment in the medial femorotibial joint according to their positions in embedded joints (Fig. 1). The posterior femur (FP) and posterior tibia (TP) were defined as the regions of articular cartilage located between the inner edges of the anterior and posterior meniscal horns. The edges of the anterior femoral (FA) and anterior tibial (TA) regions were located beyond the outer edges of the anterior meniscal horn. The middle femoral (FM) and middle tibial (TM) cartilage were situated between the FA and FP regions or between the TA and TP regions, and located adjacent to the anterior horn of the meniscus. In our pilot study, FM and TM regions contacted each other when the joint bent at 80° flexion [Supplementary Fig. 1(D)], which is the approximate flexion observed at the beginning of the gait in small rodents and when maximum contact pressure is expected in the load-bearing regions of the joint[38]. Results for histological assessments of articular cartilage were also expressed as the mean values of these six regions.

Histomorphometric analysis

According to the modification of our previous method[39], articular cartilage thickness was measured on digitized images of histological sections stained with toluidine blue, which provides excellent color discrimination between bone and calcified cartilage, as well as a distinct basophilic line that marks the location of the tidemark[5]. Briefly, at each region, a 200 μm-long stretch of the cartilage surface was defined and the areas of the uncalcified and calcified cartilage under this stretch were measured separately. The thickness of each layer was calculated by dividing the area by 200 μm. Total cartilage thickness was the sum of the thickness of uncalcified and calcified layer. The mean thickness for each specimen was derived by averaging measurements from three slides spaced 50 μm apart.

Chondrocyte density was measured on the sections stained with Weigert's iron hematoxylin. The cartilage area was measured using the same method as cartilage thickness, and cells with visible nuclei in the area were counted manually. Chondrocyte density was determined as the number of chondrocytes per cartilage area.

Histochemical Analysis

Alkaline phosphatase (ALP) and tartrate-resistant acid phosphatase (TRAP) activity

were detected according to the manufacturers' instructions (Sigma, St. Louis, MO, USA), and these sections were counterstained with eosin or Alcian blue, respectively. ALP-positive chondrocytes were counted manually at each cartilage region. TRAP-stained histological images were split into separate channels, and TRAP-positive cells at the entire epiphysis were identified on the red channel grayscale images by a certain threshold, using Image J 1.50 (National Institutes of Health, Bethesda, MD, USA). The TRAP-positive area per total area was calculated. In addition, osteoclast surface reaching articular cartilage was traced manually and the length was measured. The values were normalized by the length of osteochondral junction.

Immunohistochemical Analysis

Following the protocols established in our laboratory[40], sections were immunostained using antibody against type II collagen (diluted 1:150, ab21291; Abcam, Tokyo, Japan), aggrecan (diluted 1:400, AB1031; Millipore, Billerica, MA, USA), matrix metalloproteinase 13 (MMP13; diluted 1:100, AB8120; Millipore), a disintegrin and metalloproteinase with thrombospondin motifs 5 (ADAMTS5; diluted 1:75, ab41037; Abcam), type X collagen (diluted 1:1000, LB-0092; LSL, Tokyo, Japan), vascular endothelial growth factor (VEGF; diluted 1:400, ABS82; Millipore), receptor activator of nuclear factor

kappa-B ligand (RANKL; diluted 1:100, sc-7628; Santa Cruz, Dallas, TX, USA), and osteoprotegerin (OPG; diluted 1:100, ab73400; Abcam). Immunoreactivity was visualized with 3,3'-diaminobenzidine tetrahydrochloride (K3466; Dako Japan, Tokyo, Japan). On undecalcified frozen sections prepared using Kawamoto's film method, hematoxylin stains calcified tissues[37]. Therefore we used hematoxylin as counter staining in order to distinguish calcified region (deep zone of articular cartilage where calcified cartilage occupies more) and uncalcified region.

For type II collagen and aggrecan, histological images were converted to grayscale images with Adobe Photoshop CS2 (Adobe Systems, San Jose, CA, USA). The mean of pixel gray values (in the range 0 to 255) was measured with image J. Staining intensity was calculated by the following formula: Staining intensity = 255 – mean gray value

For MMP13, ADAMTS5, type X collagen, VEGF, RANKL, and OPG, the number of immune-positive cells was manually counted. Dividing the number of RANKL-positive cells by the number of OPG-positive cells, RANKL/OPG ratio was calculated.

Statistical Analysis

Statistical analyses were conducted with SPSS (IBM developer Works, Japan. IBM SPSS statistical 23). First, all data were checked for normality with the Shapiro-Wilk test. When normality was observed in all assays, the results were compared among all groups with the ANOVA test followed by the Tukey HSD test. All values are presented here as mean ± standard deviation (SD). *P* values less than 0.05 were considered significant.

Result

Microstructure of Articular Surface

The articular cartilage of femoral condyle and tibial plateau in both the experimental groups were intact macroscopically [Supplementary Fig. 2(A)]. The appearance of the cartilage surface by SEM also showed no differences among the groups [Supplementary Fig. 2(B)].

Cartilage Thickness and chondrocyte density

Cartilage matrix staining to toluidine blue, which reflect proteoglycan content, was decreased at uncalcified cartilage at posterior regions in the HU group and anterior regions in

the IM group [Fig. 2(A)]. Mean cartilage thickness of the six regions are shown in Fig. 2(B). Uncalcified cartilage of the HU group (2 weeks, 43.9 ± 2.0 μm; 4 weeks, 40.8 ± 1.1 μm; 8 weeks, 37.9 ± 2.2 μm) and the IM group (2 weeks, 43.1 ± 2.5 μm; 4 weeks, 40.0 ± 1.0 μm; 8 weeks, 35.7 ± 3.1 μm) were significantly decrease at all time points, when compared to the control group (49.9 ± 2.5 μm, $P < 0.01$). Moreover, thickness in total layer of articular cartilage were significantly decreased at 8 weeks in the HU group (97.2 ± 2.7 μm) and at 4 and 8 weeks in the IM group (4 weeks, 100.6 ± 4.8 μm; 8 weeks, 93.8 ± 8.2 μm), when compared with the control group (116.5 ± 4.0 μm, $P < 0.01$). Notably, the thickness in total and uncalcified layer at TP region in the IM group were not different from the control group at any time points (Supplementary Table 1).

Chondrocyte density in the HU group was comparable to that in the control group and normal appearance of the nuclei was observed [Fig. 2(C and D)]. In the IM group, on the other hand, significantly less cellularity was detected at all time points (versus control, $P < 0.01$). The group showed chondrocytic lacunae with picnotic or absent nuclei at FA, FM, TA, and TM region and decreased intensity of nuclear staining at FP and TP regions. Cell clusters were not found.

Cartilage Matrix and Proteases

As disclosed by immunohistochemistry, type II collagen was evenly distributed throughout the cartilage [Fig. 3(A)], and the staining intensity showed no differences among the groups [Fig. 3(B)]. The expression of MMP13, which is the most active in cleaving type II collagen, were barely detectable in chondrocytes at calcified layer [Fig. 3(A)]. Although the number of MMP13-positice cells showed no differences among the groups [Fig. 3(B)], immunoreactivity for MMP13 was also present at the bone surface corresponding to the lower edges of articular cartilage in both the experimental groups.

The control cartilage showed strong immunostaining for aggrecan, the major proteoglycan in cartilage, uniformly across the entire cartilage [Fig. 3(C)]. The experimental groups exhibited significantly less staining at uncalcified cartilage at 2 weeks (versus control, $P < 0.01$) [Fig. 3(D)]. ADAMTS5, the major aggrecanase in mouse cartilage, was distributed within chondrocytes in the control group, whereas both secreted and nuclear-localized cellular ADAMTS5 were detected in the experimental groups [Fig. 3(C)]. ADAMTS5-positive cells at uncalcified cartilage were increased at all time points in the HU group and 2 weeks in the IM group (versus control, $P < 0.05$) [Fig. 3(D)].

ALP activity and Hypertrophic Chondrocyte Markers

311

312 ALP activity, which is involved in regulating mineralization of cartilage and bone[41],
313 was located in chondrocytes on tidemark and at calcified cartilage in the control group [Fig. 4
314 (A)]. The number of ALP-positive cells were not changed at total layer. However, the number
315 showed significant increase at uncalcified layer and decrease at calcified layer in the
316 experimental groups (versus control, $P < 0.05$) [Fig. 4(B)].

317

318 The expression of type X collagen, specific marker of chondrocyte hypertrophy, was
319 observed only at cells in calcified cartilage in all groups [Fig. 4(A)]. The number of type X
320 collagen-positive cells was not different among the groups [Fig. 4(B)]. Similarly, VEGF,
321 which is synthesized by hypertrophic chondrocytes, were strongly expressed in chondrocytes
322 at calcified layer [Fig. 4(A)]. The number of VEGF-positive cells was decreased at total and
323 uncalcified layer in the experimental groups (versus control, $P < 0.05$), but showed no
324 differences at calcified layer among the groups [Fig. 4(B)].

325

326 *Bone Structure and osteoclast activity*

327

328 On μCT images, Trabecular bone was appeared to be decreased at the entire
329 epiphysis in the HU group, while the bone loss was evident at the anterior area in the IM

group [Fig. 5(A)]. BV/TV were significantly decreased in the HU group (2 weeks, 45.9 ± 5.3%; 4 weeks, 52.6 ± 2.9%; 8 weeks, 47.2 ± 1.3%) and the IM group (2 weeks, 40.4 ± 7.7%; 4 weeks, 41.6 ± 1.6%; 8 weeks, 46.6 ± 8.5%) when compared to the control group (59.9 ± 3.1%; $P < 0.05$) [Fig. 5(B)].

Histological images of the epiphysis showed similar findings of bone atrophy and expanded subchondral bone marrow space reached the articular cartilage [Fig. 5 (C)]. TRAP staining as an indicator of osteoclastic activity revealed that increased bone resorption occurred at entire epiphysis [Fig. 5(D)]. Subchondral bone loss with concomitant marrow expansion predisposed osteoclast activity at bone surface to invade into articular cartilage. Percentage of TRAP-positive area in the epiphyseal region and osteoclast surface reaching articular cartilage were markedly increased at 2 weeks in both the experimental groups when compared to the control group ($P < 0.05$) [Fig. 5(E and F)].

Immunohistochemistry revealed protein expressions of RANKL and OPG at articular chondrocytes [Supplementary Fig. 3(A)]. The number of RANKL-positive chondrocytes were increased in the HU group (versus control, $P < 0.05$) [Supplementary Fig. 3(B)]. Furthermore, both the experimental groups showed significant decrease in the number of OPG-positive chondrocytes at calcified layer (versus control, $P < 0.05$). RANKL/OPG

ratio at calcified layer increased 3.5-fold in the HU group and 3.1-fold in the IM group.

Discussion

This study demonstrated that reduced loading by the absence of weight bearing or external fixation led to decreased thickness of both the total and uncalcified layer of articular cartilage. The aggrecan content was decreased and ADAMTS5 expression was increased at uncalcified cartilage after joint unloading or immobilization, but unloading did not alter the chondrocyte density, distribution, and morphology, indicating the loss of aggrecan results from altered chondrocyte metabolism rather than apoptosis. No changes in the distributions of type X collagen imply that the cartilage thinning and matrix loss by mechanical unloading may not be mediated by hypertrophic differentiation of chondrocytes. TRAP activity penetrating into the articular cartilage associated with subchondral bone atrophy represents cartilage resorption by osteoclasts and may contribute to the cartilage thinning. Increased RANKL/OPG ratio in articular chondrocytes may be partly responsible for the subchondral osteoclast activation. Reduced ALP activity at calcified cartilage suggest suppressed mineralization at the layer and may promote further expansion of subchondral marrow. Our findings of no fibrillation at the articular surface support the notion that the cartilage alterations observed in this study is not due to overloading or shear stress, but results from

368 decreased mechanical stress.

369

370 After hindlimb unloading, uncalcified layer of articular cartilage was thinned at 2
371 weeks, whereas total layer at 8 weeks. These results indicate that 4 or less weeks of
372 experimental period are too short to detect changes in total thickness of articular cartilage
373 following joint unloading, which may explain the discordances among the results in earlier
374 studies[5,30-32]. TP region, which was the dominant weight bearing area in tibia of the fixed
375 knee joint [Supplementary Fig. 1(D)], showed no changes in cartilage thickness throughout
376 the experiment after joint immobilization. This finding supports the Carter's theory that
377 cyclic hydrostatic forces generated through joint loading maintain articular cartilage
378 thickness[42].

379

380 Some animal studies of joint unloading have reported reduction in safranin O or
381 toluidine blue staining at articular cartilage[29,31,32], indicating the loss of proteoglycans. Our
382 results suggest that mechanical unloading elicits aggrecan degradation through increased
383 expression of ADAMTS5. Uncoupling of systemic type II collagen synthesis and degradation
384 after hindlimb unloading has been reported, where serum pCol-II-C and urinary CTx-II levels
385 were analyzed[31]. Although these biomarkers have been developed to evaluate turnover of
386 type II collagen, they have low specificity. In this study, we directly analyzed the

distributions of type II collagen in the knee articular cartilage after joint unloading or immobilization and confirmed that no changes occurred. Our results imply that the loss of proteoglycans is more severe than or precede collagen alterations under unloading condition.

In OA pathogenesis, upregulation of matrix-degrading enzymes following chondrocyte hypertrophy contributes to cartilage destruction[43]. We observed increased expression of ADAMTS5 and loss of aggrecan at uncalcified cartilage. Nevertheless, the distributions of hypertrophic chondrocyte markers remained unchanged. These results indicate the possible existence of mechanism not via chondrocyte hypertrophy by which reduced load induces matrix degradation. Chondrocyte apoptosis, which increases in osteoarthritic cartilage[43], contributes to the risk of articular cartilage degeneration via its role in extracellular matrix production and maintenance. Morphological changes of articular chondrocytes have been commonly reported to be observed after joint immobilization[8-17], whereas not after joint unloading without motion restriction[29]. Our results are congruent with these reports. However, a recent study[30] demonstrated that 2 weeks of hindlimb unloading resulted in a marked increase in apoptotic chondrocytes and inducible nitric oxide synthase-positive chondrocytes in rats. Further investigations are warranted to determine whether reduced mechanical loading affect chondrocyte survival.

406 It is well accepted that disuse bone atrophy arises from increase in bone resorption
407 and/or decrease in bone formation[44]. Both joint unloading and immobilization showed a
408 significant decrease in bone volume density and a marked increase in TRAP activity at entire
409 epiphysis including subchondral bone in this study. RANKL and OPG, which are known to
410 be key molecules in the regulation of osteoclast activity, are generally produced by
411 osteoblasts/stromal cells, as well as chondrocytes[45]. Increase in RANKL/OPG ratio at
412 calcified cartilage after joint unloading or immobilization may partly contribute to osteoclast
413 activation at subchondral bone. Mature osteoclasts have shown to be capable of expression of
414 MMPs[46] and cartilage matrix resorption[47]. We found MMP13 activity distributed at the bone
415 surface corresponding to the lower edge of articular cartilage and TRAP activity invasion into
416 articular cartilage, which may represent matrix degradation and resorption by osteoclasts.
417 These findings support the concept that thinning of articular cartilage by mechanical
418 unloading is the result of osteoclastic cartilage resorption. ALP activity is required for
419 preparation of mineralization[48], and generally localized to hypertrophic cells in cartilage[49], as
420 shown in the control mice of this study. Decrease in ALP-positive cells at calcified cartilage
421 in the experimental groups represent decline in constant mineral apposition at the layer,
422 which may allow subchondral marrow expansion extend to cartilaginous layer through a
423 relative increase in bone resorption.
424

O'Connor[5], who observed mineral apposition rate at the tidemark after hindlimb unloading in rats, have attributed thinning of uncalcified cartilage by unweighting to advancement of tidemark mineralization front toward the joint surface. Subsequently, Tomiya *et al*.[31] proposed that the tidemark advancement stem largely from loss of proteoglycans, which inhibit mineralization, and that increase in ALP activity would be necessary to cause the advancement. Our findings of decreased proteoglycan content and increased ALP activity at uncalcified layer support this hypothesis of Tomiya *et al*.[31]. ALP activity is thought to localized to hypertrophic cells in cartilage[48]. Nevertheless, the distributions of ALP activity did not correspond with those of hypertrophic chondrocyte markers in the experimental groups. We showed here that chondrocytes can present ALP activity without hypertrophic differentiation and ALP activity is not necessarily localized to hypertrophic chondrocytes. However, how mechanical unloading modulates ALP activity in chondrocytes warrants future examination.

A major limitation of the present study was that the effects of aging cannot be ruled out since we had no age-matched controls. Although it is well known that aging leads to cartilage degeneration[40], thickness of articular cartilage and structure of epiphyseal cancellous bone has reported to be not altered with aging in young C57BL/6 mice at least up to 16-weeks-old[50]. We therefore regarded 8-weeks-old mice with no intervention as control of

all experimental groups, and this approach has the advantages of minimizing the number of animals. Hindlimbs of immobilized animals exhibited slight signs of inflammation such as edema for a few days postsurgery. The secretion of inflammatory cytokines or neuroendocrine response induced by operative stress may affect the knee articular cartilage or subchondral bone. However, it has been shown that sham surgery (wire insertion without external fixation) did not elicit cartilage degeneration[15,16].

In conclusion, we propose that mechanical unloading induces thinning of articular cartilage via acceleration of aggrecan catabolism, modulation of cartilage matrix mineralization, and subchondral osteoclast activation (Fig. 6). Reduced loading did not affect specific markers for chondrocyte hypertrophy and therefore may induces cartilage degeneration in a different manner than overloading, suggesting that the vast body of knowledge already gained from studies on OA cannot be fully applied to cartilage degeneration by disuse.

Acknowledgements

We would like to acknowledge Dr. Momoko Nagai for advises on the surgical immobilization. We also acknowledge the skillful technical assistance of Mr. Kosuke

Watanabe and Mr. Tomohiro Yoshikawa.

Author contributions

Conception and design of the study: MN, NS, HI, HK, and HM.

Analysis and interpretation of the data: MN, NS, HI, YK, YW, and HM.

Drafting of the article: MN.

Critical revision of the article for important intellectual content: HM.

Final approval of the article: all co-authors.

Statistical expertise: MN, YK, and HM.

Obtaining of funding: HM.

Collection and assembly of data: MN, NS, HI, YK, and ST.

Role of the funding source

This study was supported in part by Japan Society for the Promotion of Science (JSPS) KAKENHI Grant Number 25702032.

Competing interest statement

The authors have no conflicts of interest to disclose.

References

1. Madry H, Luyten FP, Facchini A. Biological aspects of early osteoarthritis. Knee Surg Sports Traumatol Arthrosc 2012;20:407-22.
2. Bleuel J, Zaucke F, Brüggemann GP, Niehoff A. Effects of cyclic tensile strain on chondrocyte metabolism: a systematic review. PLoS One 2015;10:e0119816.
3. Silverwood V, Blagojevic-Bucknall M, Jinks C, Jordan JL, Protheroe J, Jordan KP. Current evidence on risk factors for knee osteoarthritis in older adults: a systematic review and meta-analysis. Osteoarthritis Cartilage 2015;23:507-15.
4. Vanwanseele B, Lucchinetti E, Stüssi E. The effects of immobilization on the characteristics of articular cartilage: current concepts and future directions. Osteoarthritis Cartilage 2002;10:408-19.
5. O'Connor KM. Unweighting accelerates tidemark advancement in articular cartilage at the knee joint of rats. J Bone Miner Res 1997;12:580-9.
6. Iqbal K, Khan Y, Minhas LA. Effects of immobilization on thickness of superficial zone of articular cartilage of patella in rats. Indian J Orthop 2012;46:391-4.
7. Kiviranta I, Jurvelin J, Tammi M, Säämänen AM, Helminen HJ. Weight bearing controls glycosaminoglycan concentration and articular cartilage thickness in the knee joints of young beagle dogs. Arthritis Rheum 1987;30:801-9.

8. Maldonado DC, Silva MC, Neto Sel-R, de Souza MR, de Souza RR. The effects of joint immobilization on articular cartilage of the knee in previously exercised rats. J Anat 2013;222:518-25.
9. Sood SC. A study of the effects of experimental immobilisation on rabbit articular cartilage. J Anat 1971;108:497-507.
10. Palmoski M, Perricone E, Brandt KD. Development and reversal of a proteoglycan aggregation defect in normal canine knee cartilage after immobilization. Arthritis Rheum 1979;22:508-17.
11. Paukkonen K, Jurvelin J, Helminen HJ. Effects of immobilization on the articular cartilage in young rabbits. A quantitative light microscopic stereological study. Clin Orthop Relat Res 1986;206:270-80.
12. Trudel G, Himori K, Uhthoff HK. Contrasting alterations of apposed and unapposed articular cartilage during joint contracture formation. Arch Phys Med Rehabil 2005;86:90-7.
13. Ando A, Hagiwara Y, Chimoto E, Hatori K, Onoda Y, Itoi E. Intra-articular injection of hyaluronan diminishes loss of chondrocytes in a rat immobilized-knee model. Tohoku J Exp Med 2008;215:321-31.
14. Hagiwara Y, Ando A, Chimoto E, Saijo Y, Ohmori-Matsuda K, Itoi E. Changes of articular cartilage after immobilization in a rat knee contracture model. J Orthop Res

2009;27:236-42.

15. Nagai M, Ito A, Tajino J, Iijima H, Yamaguchi S, Zhang X, *et al*. Remobilization causes site-specific cyst formation in immobilization-induced knee cartilage degeneration in an immobilized rat model. J Anat 2016;228:929-39.

16. Nagai M, Aoyama T, Ito A, Tajino J, Iijima H, Yamaguchi S, *et al*. Alteration of cartilage surface collagen fibers differs locally after immobilization of knee joints in rats. J Anat 2015;226:447-57.

17. Thaxter TH, Mann RA, Anderson CE. Degeneration of immobilized knee joints in rats; histological and autoradiographic study. J Bone Joint Surg Am 1965;47:567-85.

18. Behrens F, Kraft EL, Oegema TR Jr. Biochemical changes in articular cartilage after joint immobilization by casting or external fixation. J Orthop Res 1989;7:335-43.

19. Jortikka MO, Inkinen RI, Tammi MI, Parkkinen JJ, Haapala J, Kiviranta I, *et al*. Immobilisation causes longlasting matrix changes both in the immobilised and contralateral joint cartilage. Ann Rheum Dis 1997;56:255-61.

20. Slowman SD, Brandt KD. Composition and glycosaminoglycan metabolism of articular cartilage from habitually loaded and habitually unloaded sites. Arthritis Rheum 1986;29:88-94.

21. Säämänen AM, Tammi M, Jurvelin J, Kiviranta I, Helminen HJ. Proteoglycan alterations following immobilization and remobilization in the articular cartilage of young canine

knee (stifle) joint. J Orthop Res 1990;8:863-73.

22. Videman T, Eronen I, Friman C. Glycosaminoglycan metabolism in experimental osteoarthritis caused by immobilization. The effects of different periods of immobilization and follow-up. Acta Orthop Scand 1981;52:11-21.

23. Videman T, Eronen I, Candolin T. [3H]proline incorporation and hydroxyproline concentration in articular cartilage during the development of osteoarthritis caused by immobilization. A study in vivo with rabbits. Biochem J 1981;200:435-40.

24. Hagiwara Y, Ando A, Chimoto E, Tsuchiya M, Takahashi I, Sasano Y, *et al*. Expression of collagen types I and II on articular cartilage in a rat knee contracture model. Connect Tissue Res 2010;51:22-30.

25. Langenskiöld A, Michelsson JE, Videman T. Osteoarthritis of the knee in the rabbit produced by immobilization. Attempts to achieve a reproducible model for studies on pathogenesis and therapy. Acta Orthop Scand 1979;50:1-14.

26. Józsa L, Järvinen M, Kannus P, Réffy A. Fine structural changes in the articular cartilage of the rat's knee following short-term immobilisation in various positions: a scanning electron microscopical study. Int Orthop 1987;11:129-33.

27. Jurvelin J, Helminen HJ, Lauritsalo S, Kiviranta I, Säämänen AM, Paukkonen K, *et al*. Influences of joint immobilization and running exercise on articular cartilage surfaces of young rabbits. A semiquantitative stereomicroscopic and scanning electron microscopic

560 study. Acta Anat (Basel) 1985;122:62-8.
561 28. Ando A, Hagiwara Y, Tsuchiya M, Onoda Y, Suda H, Chimoto E, *et al*. Increased
562 expression of metalloproteinase-8 and -13 on articular cartilage in a rat immobilized knee
563 model. Tohoku J Exp Med 2009;217:271-8.
564 29. Palmoski MJ, Colyer RA, Brandt KD. Joint motion in the absence of normal loading
565 does not maintain normal articular cartilage. Arthritis Rheum 1980;23:325-34.
566 30. Basso N, Heersche JN. Effects of hind limb unloading and reloading on nitric oxide
567 synthase expression and apoptosis of osteocytes and chondrocytes. Bone 2006;39:807-
568 14.
569 31. Tomiya M, Fujikawa K, Ichimura S, Kikuchi T, Yoshihara Y, Nemoto K. Skeletal
570 unloading induces a full-thickness patellar cartilage defect with increase of urinary
571 collagen II CTx degradation marker in growing rats. Bone 2009;44:295-305.
572 32. Luan HQ, Sun LW, Huang YF, Wu XT, Niu H, Liu H, *et al*. Use of micro-computed
573 tomography to evaluate the effects of exercise on preventing the degeneration of articular
574 cartilage in tail-suspended rats. Life Sci Space Res (Amst) 2015;6:15-20.
575 33. Hinterwimmer S, Krammer M, Krötz M, Glaser C, Baumgart R, Reiser M, *et al*.
576 Cartilage atrophy in the knees of patients after seven weeks of partial load bearing.
577 Arthritis Rheum 2004;50:2516-20.
578 34. Ferreira JA, Crissey JM, Brown M. An alternant method to the traditional NASA

579 hindlimb unloading model in mice. J Vis Exp 2011;49:2467.
580 35. Hargens AR, Steskal J, Johansson C, Tipton CM. Tissue fluid shift, forelimb loading, and
581 tail tension in tail-suspended rats. Physiologist 1984;27:37-8.
582 36. Nagai M, Aoyama T, Ito A, Iijima H, Yamaguchi S, Tajino J, *et al*. Contributions of
583 biarticular myogenic components to the limitation of the range of motion after
584 immobilization of rat knee joint. BMC Musculoskelet Disord 2014;15:224.
585 37. Kawamoto T, Kawamoto K. Preparation of thin frozen sections from nonfixed and
586 undecalcified hard tissues using Kawamot's film method (2012). Methods Mol Biol
587 2014;1130:149-64.
588 38. Das Neves Borges P, Forte AE, Vincent TL, Dini D, Marenzana M. Rapid, automated
589 imaging of mouse articular cartilage by microCT for early detection of osteoarthritis and
590 finite element modelling of joint mechanics. Osteoarthritis Cartilage 2014;22:1419-28.
591 39. Moriyama H, Yoshimura O, Kawamata S, Takayanagi K, Kurose T, Kubota A, *et al*.
592 Alteration in articular cartilage of rat knee joints after spinal cord injury. Osteoarthritis
593 Cartilage 2008;16:392-8.
594 40. Moriyama H, Kanemura N, Brouns I, Pintelon I, Adriaensen D, Timmermans JP, *et al*.
595 Effects of aging and exercise training on the histological and mechanical properties of
596 articular structures in knee joints of male rat. Biogerontology 2012;13:369-81.
597 41. Bellows CG, Heersche JN, Aubin JE. Inorganic phosphate added exogenously or

released from beta-glycerophosphate initiates mineralization of osteoid nodules in vitro. Bone Miner 1992;17:15-29.

42. Carter DR, Wong M. The role of mechanical loading histories in the development of diarthrodial joints. J Orthop Res 1988;6:804-16.

43. Husa M, Liu-Bryan R, Terkeltaub R. Shifting HIFs in osteoarthritis. Nat Med 2010;16:641-4.

44. Dehority W, Halloran BP, Bikle DD, Curren T, Kostenuik PJ, Wronski TJ, *et al*. Bone and hormonal changes induced by skeletal unloading in the mature male rat. Am J Physiol 1999;276:62-9.

45. Funck-Brentano T, Cohen-Solal M. Crosstalk between cartilage and bone: when bone cytokines matter. Cytokine Growth Factor Rev. 2011;22:91-7.

46. Andersen TL, del Carmen Ovejero M, Kirkegaard T, Lenhard T, Foged NT, Delaissé JM. A scrutiny of matrix metalloproteinases in osteoclasts: evidence for heterogeneity and for the presence of MMPs synthesized by other cells. Bone 2004;35:1107-19.

47. Knowles HJ, Moskovsky L, Thompson MS, Grunhen J, Cheng X, Kashima TG, *et al*. Chondroclasts are mature osteoclasts which are capable of cartilage matrix resorption. Virchows Arch 2012;461:205-10.

48. Roach HI. Association of matrix acid and alkaline phosphatases with mineralization of cartilage and endochondral bone. Histochem J 1999;31:53-61.

49. Miao D, Scutt A. Histochemical localization of alkaline phosphatase activity in decalcified bone and cartilage. J Histochem Cytochem 2002;50:333-40.

50. Ko FC, Dragomir C, Plumb DA, Goldring SR, Wright TM, Goldring MB, *et al*. In vivo cyclic compression causes cartilage degeneration and subchondral bone changes in mouse tibiae. Arthritis Rheum 2013;65:1569-78.

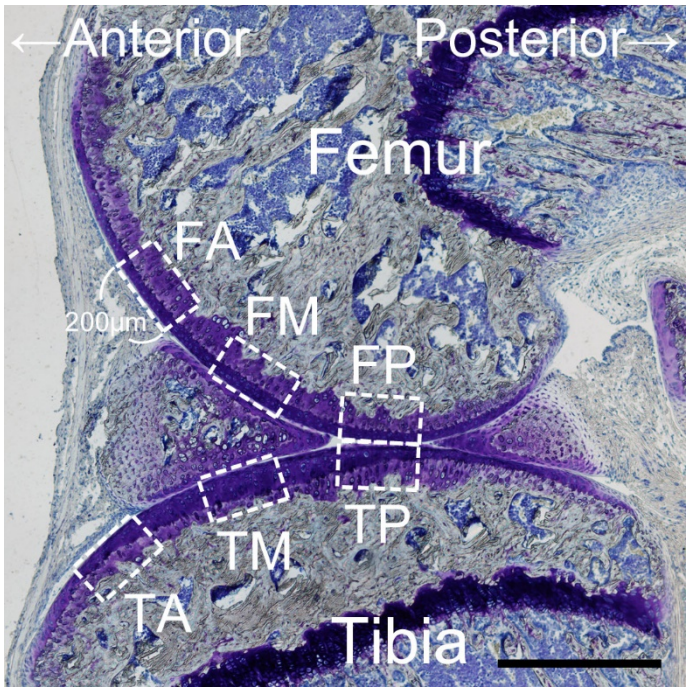

Fig. 1. Knee cartilage regions for histological evaluation were determined on sagittal section at the medial midcondylar level. Assessment was perfomed at each region of 200 μm in width. Toluidine blue staining. Scale bar = 500 μm. Cartilage region: FA, FM, FP, TA, TM, and TP.

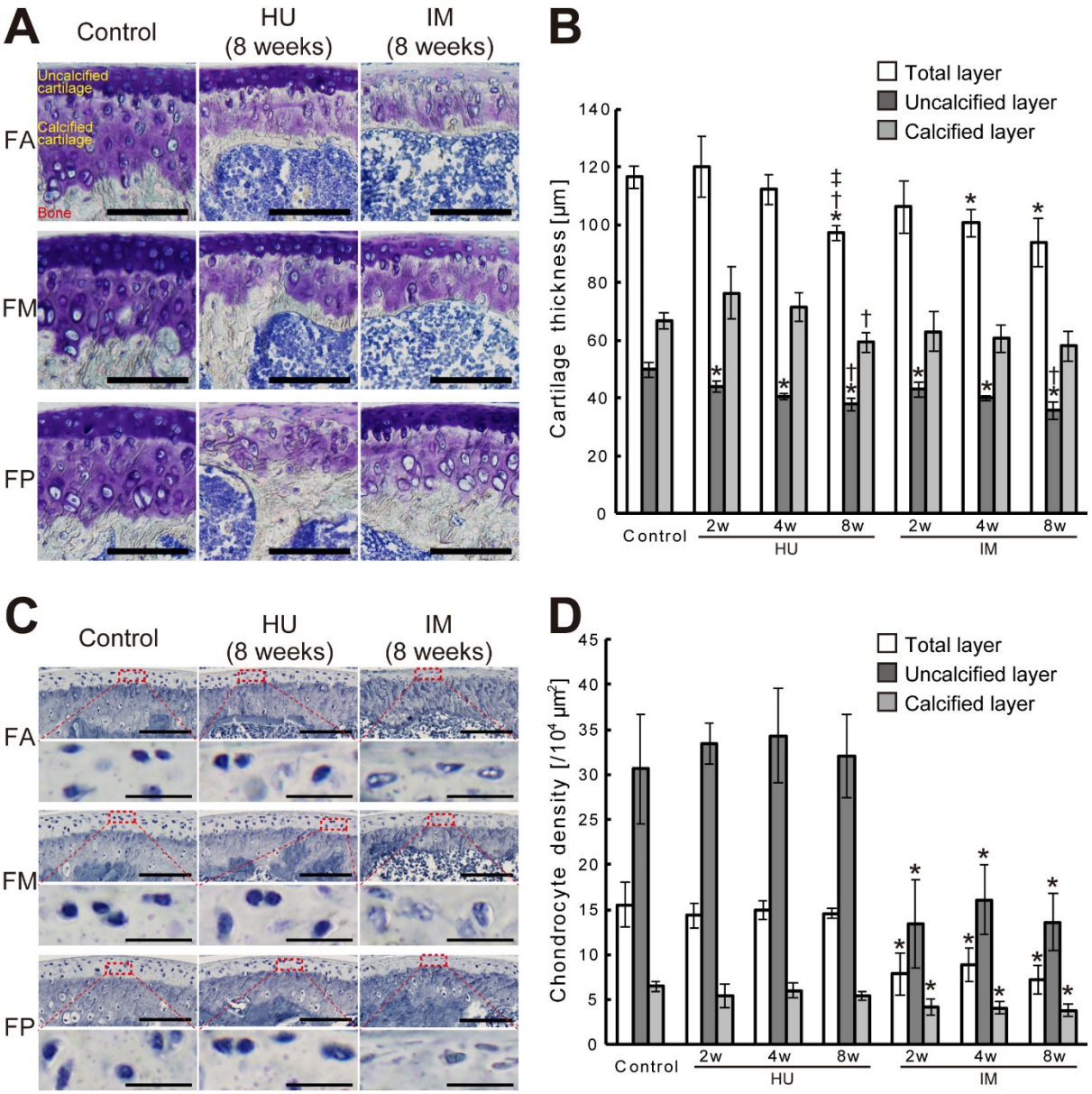

627

628 **Fig. 2.** Cartilage thickness and chondrocyte density. (A) Thickness in uncalcified and

629 calcified layer of articular cartilage were measured separately on the histological sections

630 stained with toluidine blue. Staining intensity was decreased at uncalcified layer in FP region

631 of the HU group and FA regions of the IM group. Scale bars = 100 μm. (B) Mean cartilage

632 thickness of the six regions. At 8 weeks, both of the experimental groups showed significant

633 decrease in thickness of total and uncalcified layer. Results for each region are shown in

Supplementary Table 1. (C) Histological observations of chondrocyte density (upper row; scale bars = 100 μm) and morphology (lower row, scale bars = 20 μm). Chondrocytes in the IM group showed picnotic nuclei, lacunae without nuclei, and less intensity of nuclear staining. Weigert's iron hematoxylin staining. (D) Mean chondrocyte density of the six regions. Only the IM group showed significantly less density. Results for each region are shown in Supplementary Table 2. * Significant differences from the control group. † Significant differences from the 2 weeks after the same intervention. ‡ Significant differences from the 4 weeks after the same intervention. Cartilage region: FA, FM, FP.

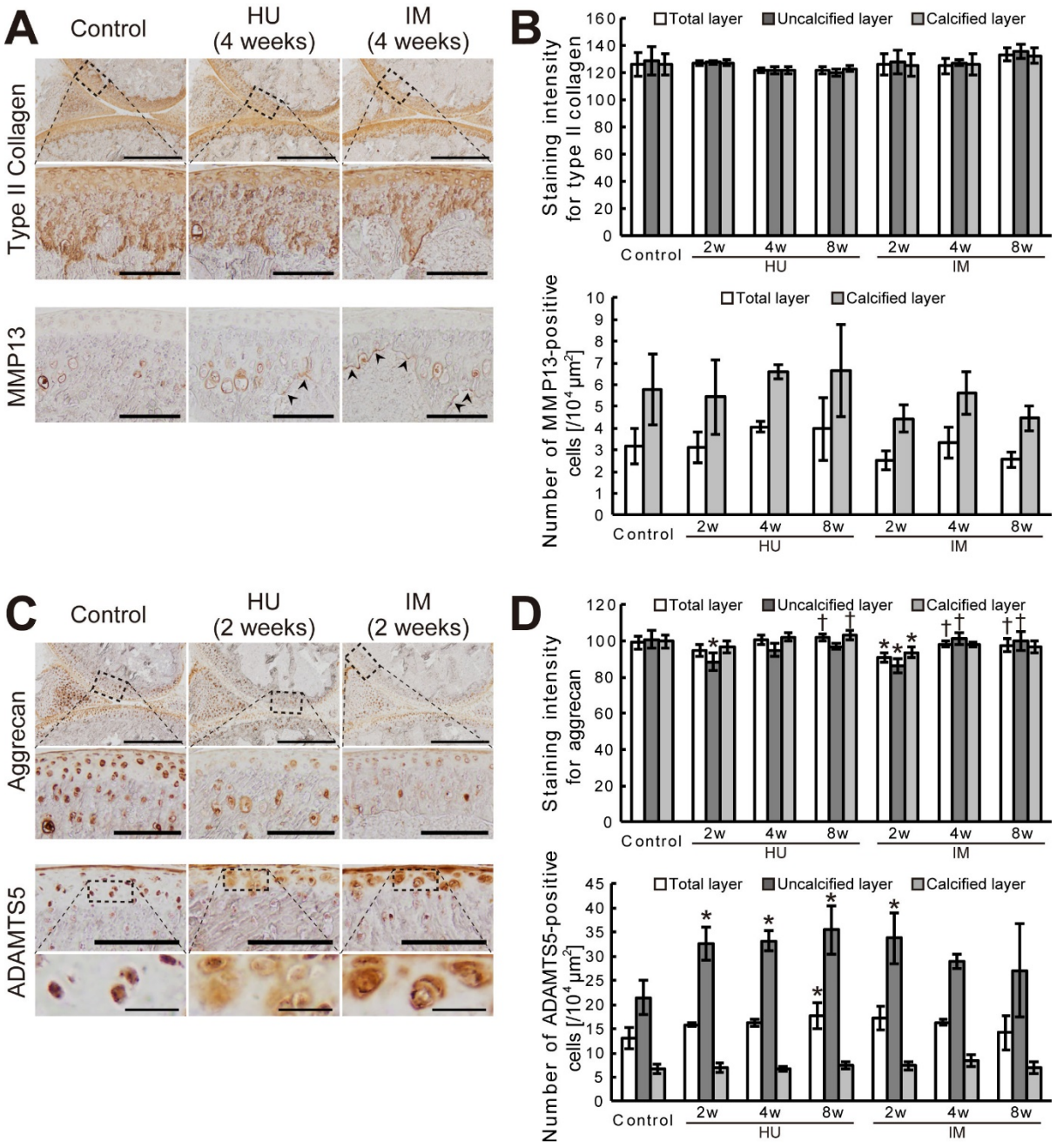

642

643 **Fig. 3.** Distributions of cartilage matrixes and expressions of matrix proteases. (A)

644 Immunostaining for type II collagen was seen strongly in articular cartilage at all regions in

645 all groups. MMP13 expression was observed in chondrocyte at calcified layer. In the HU and

646 IM groups, immunolabeling was also detected at bone surface corresponding with the lower

647 edges of articular cartilage in the HU and IM groups (arrow head). Scale bars = 500 μm

(upper row of type II collagen), 100 μm (lower row of type II collagen and MMP13). (B) Staining intensity for type II collagen and the number of MMP13-positive cells. Mean values of the six regions. Results for each region are shown in Supplementary Table 3 and 4. (C) Aggrecan was distributed throughout the whole cartilage. Higher-magnification views of the boxed areas show less intensity at uncalcified layer in the HU and IM groups. ADAMTS5 was barely detectable in chondrocytes in the control, whereas the pericellular regions of uncalcified cartilage were clearly stained in the HU and IM groups. Scale bars = 500 μm (upper row of aggrecan), 100 μm (lower row of aggrecan and upper row of ADAMTS5), 20 μm (lower row of ADAMTS5) (D) Staining intensity for aggrecan and the number of ADAMTS5-positive cells. Mean values of the six regions. Results for each region are shown in Supplementary Table 5 and 6. * Significant differences from the control group. † Significant differences from the 2 weeks after the same intervention.

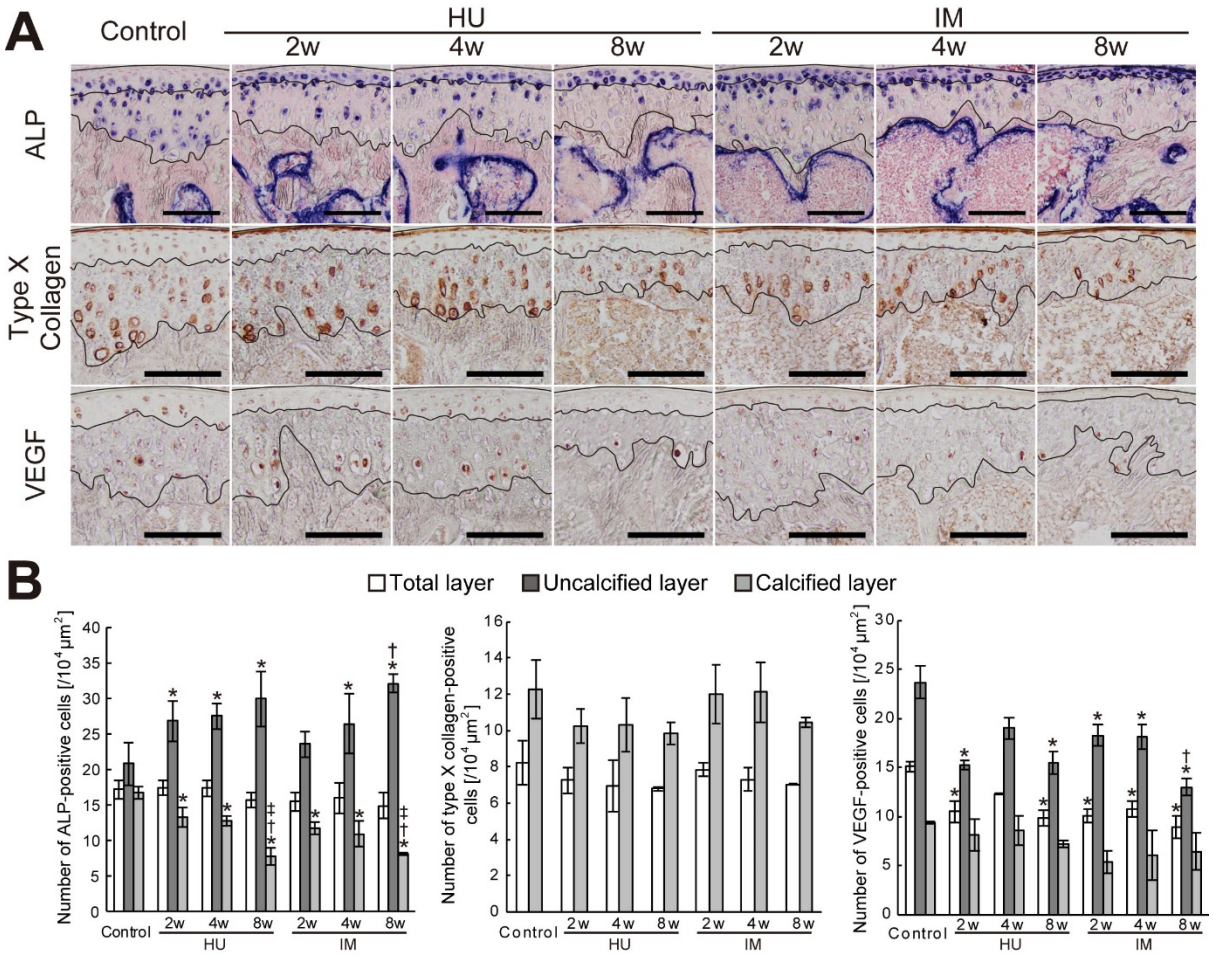

660

661 **Fig. 4.** Distributions of ALP activity and markers of chondrocyte hypertrophy. (A)

662 Progressive decrease in ALP-positive cells in calcified layer of articular cartilage were

663 observed in the HU and IM groups. Uncalcified cartilage in the IM group exhibited marked

664 increases in ALP activity. Immunostaining for type X collagen or VEGF was seen strongly at

665 calcified layer. Scale bars = 100 μm. (B) The numbers of ALP-, type X collagen-, and VEGF-

666 positive chondrocytes. Mean values of the six regions. Results for each region are shown in

667 Supplementary Table 7, 8, and 9. * Significant differences from the control group. †

668 Significant differences from the 2 weeks after the same intervention. ‡ Significant differences

669 from the 4 weeks after the same intervention.

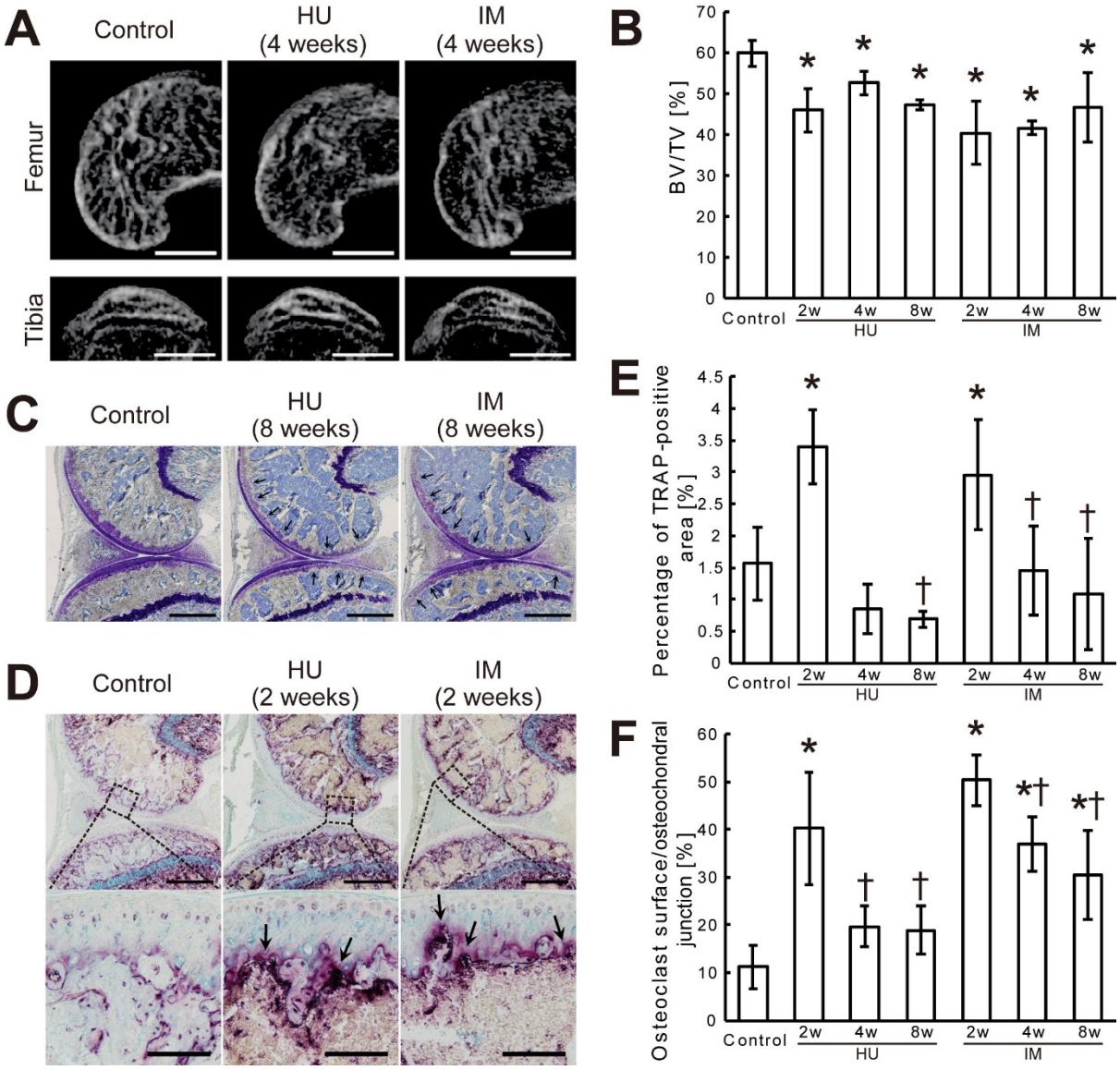

Fig. 5. Bone structure and TRAP activity. (A) 3D images of distal femur and proximal tibia obtained by μCT scanning. (B) Bone volume density (BV/TV) was quantified based on μCT data. (C) Representative histological images of the whole knee joint stained with toluidine blue. Associated with loss of trabecular and subchondral bone, expanded bone marrow space reached the articular cartilage (arrows). Scale bars = 500 μm. (D) Representative histological sections stained with TRAP/alcian blue. Scale bars = 500 μm (upper row), 100 μm (lower row). The HU and IM groups showed increased TRAP activity at entire epiphysis at 2 weeks,

678 and the activity invaded into calcified layer of articular cartilage (arrow). (E) Percentage of
679 TRAP-positive area at epiphyseal region. (F) Osteoclast surface reaching cartilaginous layer
680 per osteochondral junction. * Significant differences from the control group. † Significant
681 differences from the 2 weeks after the same intervention.

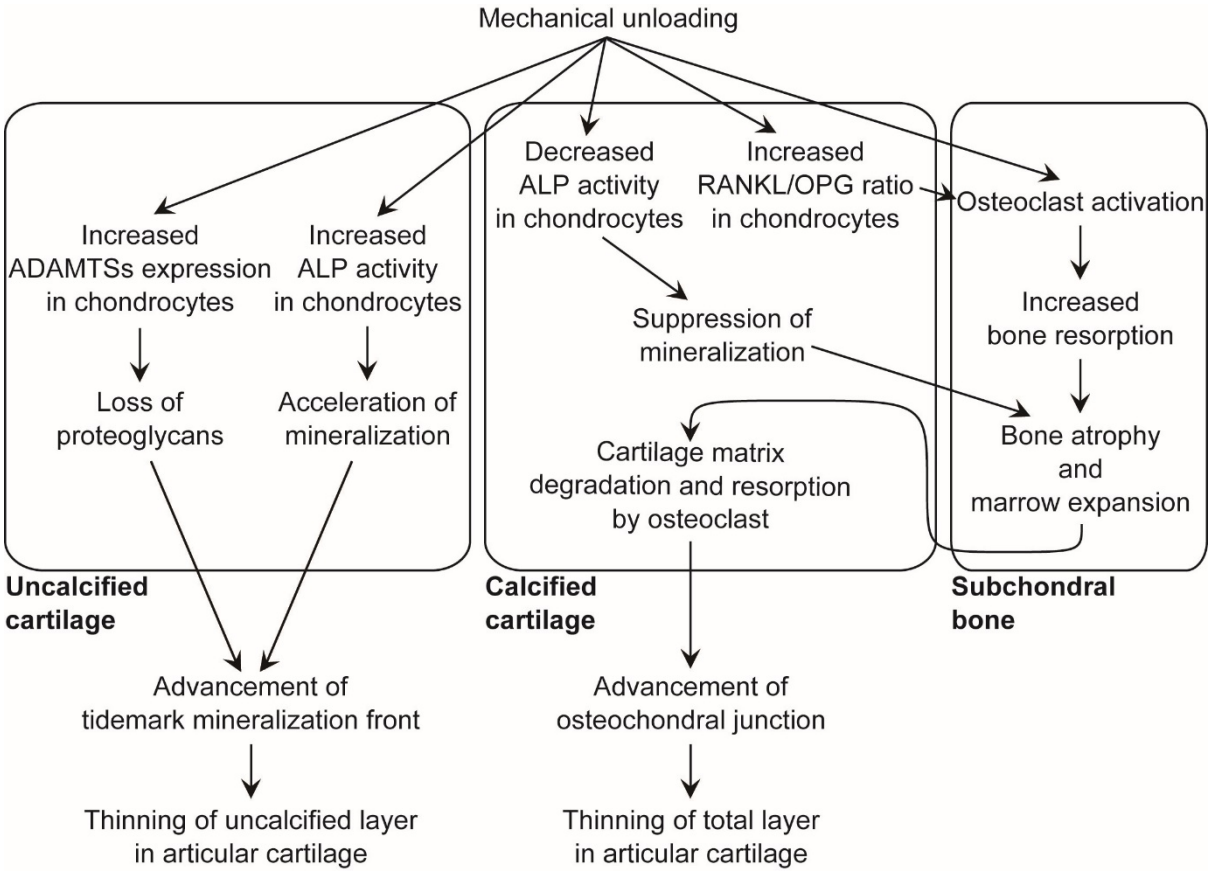

Fig. 6. Schema of unloading-induced articular cartilage thinning. Increased ALP activity with concomitant loss of proteoglycans associated with increased aggrecanase expression at uncalcified cartilage leads to tidemark advancement toward the articular surface, resulting in thinning of uncalcified layer of articular cartilage. Subchondral osteoclast activation, which is partly induced by increased RANKL/OPG ratio in articular chondrocytes, induces subchondral bone atrophy. Decreased ALP activity in chondrocytes at calcified cartilage allows subchondral marrow space to invade articular cartilage. Advancement of osteochondral junction through cartilage matrix degradation and resorption by osteoclast results in thinning of total layer in articular cartilage.

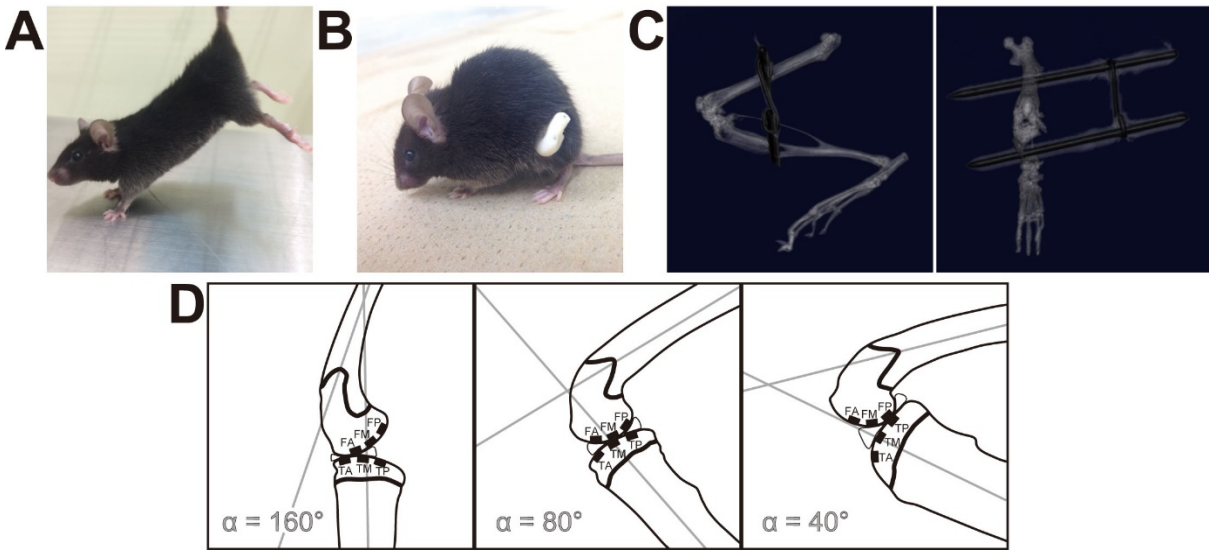

692

693 **Supplementary Fig. 1.** Animal models and relative position of the regions for assessment.

694 (A) Tail suspended mice maintained their hindlimbs at extended position. (B) Mice treated

695 with surgical immobilization of the knee joints exhibited bilaterally symmetric standing and

696 ambulation. (C) Confirmation of joint fixation. μCT scanning revealed that kirschner wires

697 penetrated through bones. (left) lateral view. (right) frontal view. (D) Positions of cartilage

698 regions when the knee joint angle (α) is 40° (maximal flexion; immobilized), 80° (typical

699 joint angle; control), 160° (maximal extension; hindlimb unloaded).

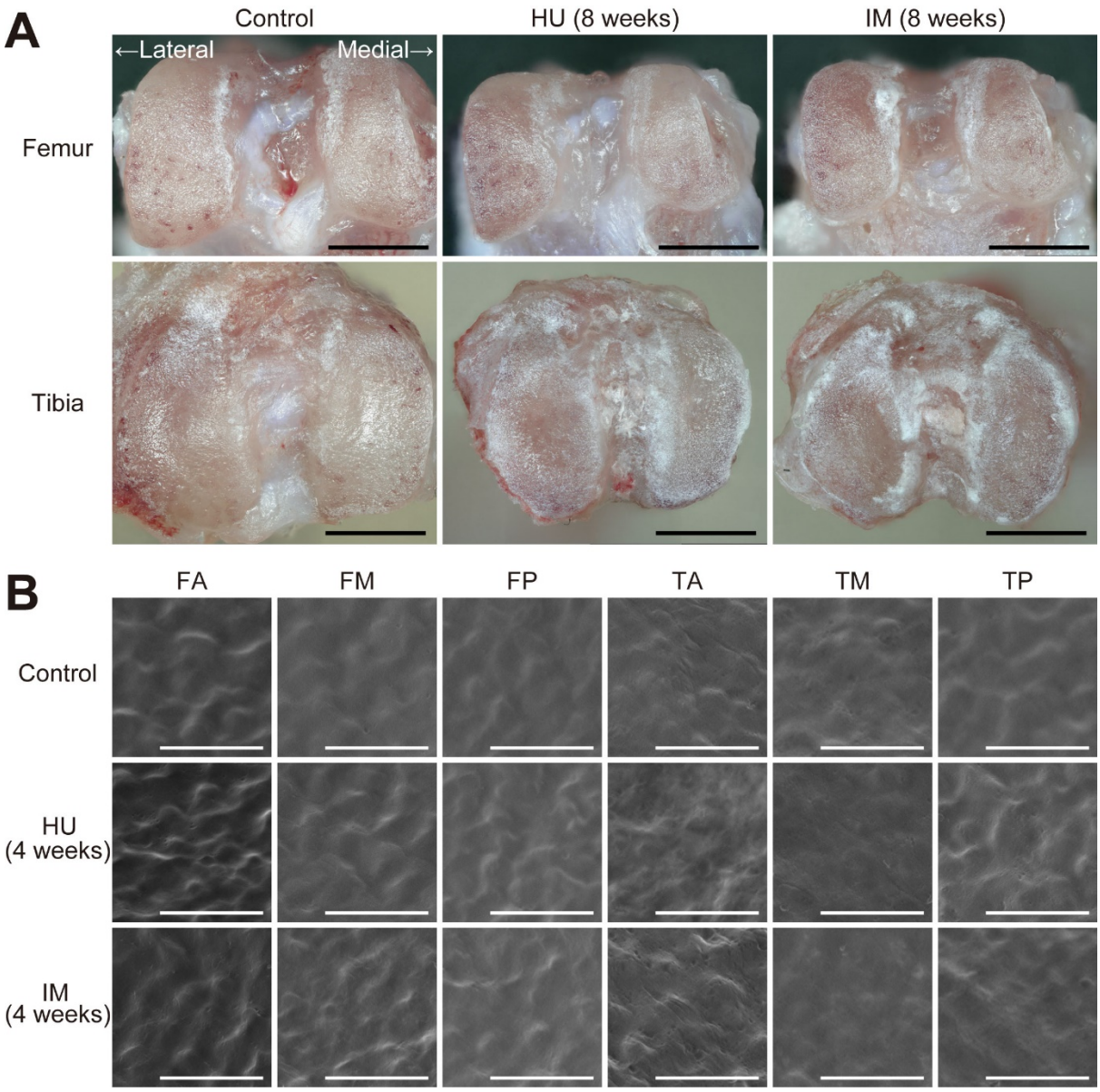

Supplementary Fig. 2. (A) Macroscopic (scale bars = 1 mm) and (B) Scanning Electron Microscopic (SEM; scale bars = 50 μm) observations of articular surface of the knee joints.

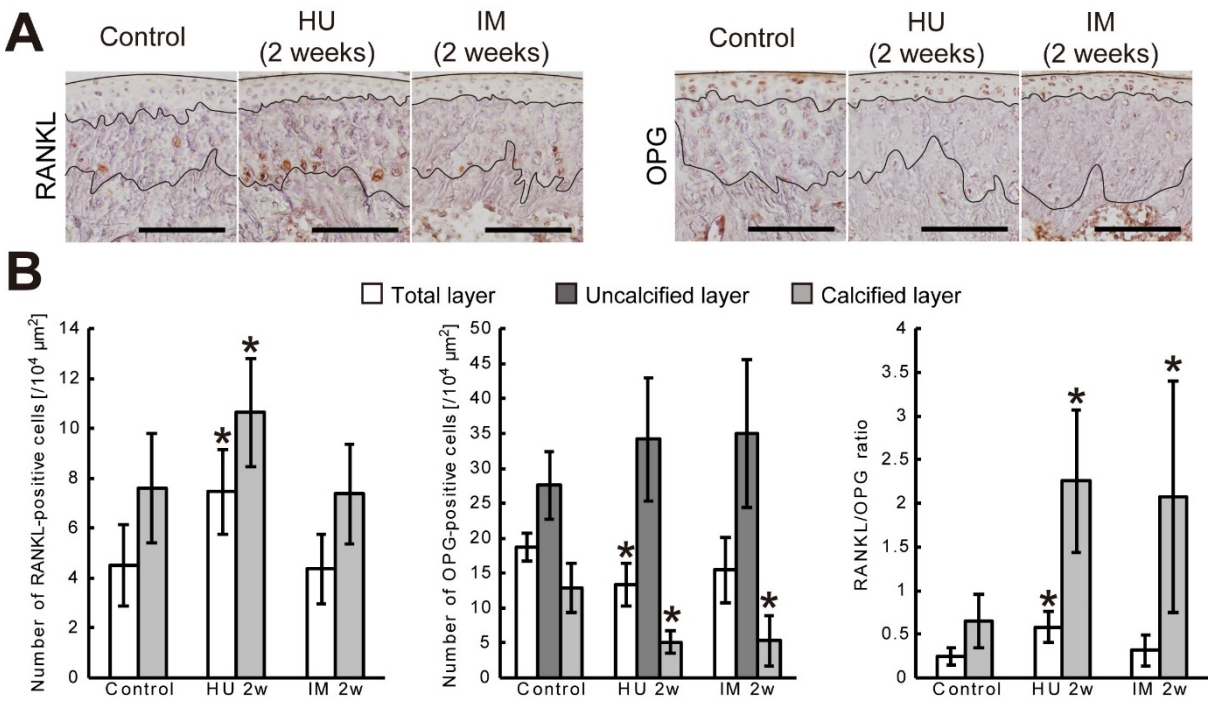

703

704 **Supplementary Fig. 3.** Expressions of RANKL and OPG in articular chondrocytes. (A)

705 Representative immunohistochemical staining images. Scale bars = 100 μm. (B) Numbers of

706 RANKL- and OPG-positive chondrocytes were counted and RANKL/OPG ratio were

707 calculated. * Significant differences from the control group.

Supplementary Table 1. Cartilage thickness (μm) at each region after hindlimb unloading or joint immobilization.

		Control	Hindlimb Unloading			Joint Immobilization		
Region	Layer		2w	4w	8w	2w	4w	8w
FA	Total	128.1 ± 9.2	126.5 ± 19.5	112.5 ± 9.9	94.7 ± 7.2*†	119.1 ± 11.0	102.2 ± 5.9*	92.7 ± 15.3*†
	Uncalcified	37.5 ± 2.6	32.3 ± 1.6*	29.2 ± 0.3*	29.4 ± 3.0*	31.8 ± 4.0	28.9 ± 3.4	27.1 ± 8.6*
	Calcified	90.5 ± 7.5	94.2 ± 18.0	83.3 ± 9.7	65.3 ± 5.0*†	87.4 ± 7.4	73.3 ± 8.4*	65.5 ± 8.8*†
FM	Total	121.2 ± 5.0	122.9 ± 18.4	115.4 ± 13.4	94.6 ± 7.0*†	104.4 ± 14.1	97.7 ± 7.8*	81.3 ± 10.2*†
	Uncalcified	44.0 ± 3.3	35.3 ± 5.3*	33.5 ± 4.2*	31.9 ± 3.7*	35.7 ± 6.8	31.9 ± 2.1*	31.2 ± 5.3*
	Calcified	77.3 ± 5.4	87.6 ± 13.9	81.8 ± 10.7	62.7 ± 10.2†	68.7 ± 7.6	65.8 ± 5.9	50.1 ± 6.6*†‡
FP	Total	112.3 ± 8.7	101.0 ± 7.5	94.3 ± 3.9*	84.7 ± 3.2*†	98.9 ± 10.3	91.5 ± 5.4	84.3 ± 18.3*
	Uncalcified	37.5 ± 2.1	26.7 ± 4.2*	30.5 ± 2.1*	28.5 ± 2.1*	35.4 ± 0.4	35.3 ± 2.1	31.5 ± 1.5*†‡
	Calcified	74.8 ± 7.0	74.3 ± 4.4	63.9 ± 4.8*	56.2 ± 2.8*†	63.4 ± 10.4	56.3 ± 4.4	52.8 ± 16.9*
TA	Total	93.5 ± 4.1	113.7 ± 9.9*	111.4 ± 4.5*	96.9 ± 8.8†‡	84.2 ± 2.4	86.1 ± 5.1	89.2 ± 11.4
	Uncalcified	46.7 ± 2.7	43.0 ± 7.0	40.4 ± 3.1	36.9 ± 3.6*	36.2 ± 1.4*	30.6 ± 5.8*	19.4 ± 4.1*†‡
	Calcified	46.9 ± 5.0	70.7 ± 4.5*	71.0 ± 4.2*	59.9 ± 12.3	48.0 ± 1.6	55.5 ± 3.3	69.7 ± 8.4*†‡
TM	Total	127.7 ± 6.7	140.3 ± 5.3*	129.6 ± 2.6†	119.7 ± 2.2†	118.5 ± 6.2	118.4 ± 5.6	112.5 ± 6.1*
	Uncalcified	85.2 ± 7.1	83.6 ± 5.2	74.8 ± 2.4*	66.5 ± 5.7*†	76.2 ± 5.5	70.1 ± 4.6*	58.4 ± 5.5*
	Calcified	42.6 ± 7.1	56.7 ± 6.2*	54.7 ± 1.6*	53.2 ± 5.1	42.2 ± 4.7	48.3 ± 5.8	54.1 ± 8.8
TP	Total	116.2 ± 7.6	117.1 ± 14.4	110.1 ± 8.9	92.5 ± 2.2*†	111.8 ± 14.4	107.5 ± 15.4	103.0 ± 4.2
	Uncalcified	48.5 ± 3.3	42.6 ± 5.4	36.4 ± 3.9*	34.0 ± 1.7*†	43.2 ± 2.6	43.3 ± 6.7	46.8 ± 4.1
	Calcified	67.7 ± 7.8	74.5 ± 13.9	73.7 ± 5.0	58.5 ± 3.3	68.7 ± 15.2	64.2 ± 16.8	56.2 ± 3.2

* Significant differences from the control group.

† Significant differences from the 2 weeks after the same intervention.

‡ Significant differences from the 4 weeks after the same intervention.

712 **Supplementary Table 2.** Chondrocyte density (/10^4 μm^2) at each region after hindlimb unloading or joint immobilization.

		Control	Hindlimb Unloading			Joint Immobilization		
Region	Layer		2w	4w	8w	2w	4w	8w
FA	Total	19.0 ± 4.3	14.1 ± 1.9	14.1 ± 1.2	14.3 ± 2.0	7.2 ± 2.3*	4.8 ± 1.4*	3.9 ± 2.0*
	Uncalcified	43.6 ± 16.2	36.1 ± 6.1	38.1 ± 7.3	35.4 ± 5.5	12.6 ± 4.4*	7.0 ± 5.1*	8.6 ± 6.5*
	Calcified	10.7 ± 1.4	7.5 ± 1.8*	5.9 ± 1.6*	5.3 ± 1.2*	5.5 ± 1.9*	3.8 ± 0.3*	2.6 ± 1.0*
FM	Total	16.4 ± 3.8	14.4 ± 1.6	14.1 ± 1.5	15.9 ± 3.6	7.5 ± 3.9*	6.1 ± 1.7*	6.2 ± 2.9*
	Uncalcified	34.9 ± 10.3	37.5 ± 3.2	35.1 ± 8.9	36.8 ± 7.2	13.7 ± 6.0*	15.3 ± 2.9*	11.1 ± 3.8*
	Calcified	7.1 ± 1.4	5.6 ± 1.5	6.6 ± 1.3	6.1 ± 2.3	4.3 ± 1.6	2.0 ± 1.5*	3.5 ± 2.5*
FP	Total	13.7 ± 4.6	13.5 ± 1.6	15.9 ± 2.6	14.0 ± 1.4	9.1 ± 1.5	10.5 ± 3.4	7.0 ± 4.4
	Uncalcified	26.4 ± 11.2	36.4 ± 8.6	39.8 ± 8.9	31.0 ± 10.3	15.3 ± 3.8	19.7 ± 7.5	12.2 ± 8.2
	Calcified	7.1 ± 2.8	5.9 ± 2.3	6.9 ± 3.0	6.2 ± 1.9	4.5 ± 1.5	5.7 ± 2.0	4.1 ± 1.5
TA	Total	15.7 ± 4.3	15.7 ± 3.5	16.3 ± 2.2	15.6 ± 2.2	4.7 ± 3.8*	6.8 ± 3.3*	8.1 ± 3.8*
	Uncalcified	28.6 ± 8.3	35.5 ± 3.9	36.0 ± 8.9	33.7 ± 3.4	7.2 ± 8.3*	10.4 ± 8.0	21.9 ± 18.2
	Calcified	3.3 ± 0.6	4.3 ± 2.1	5.2 ± 1.5	4.8 ± 1.2	3.2 ± 1.1	4.7 ± 3.6	3.1 ± 1.1
TM	Total	15.2 ± 4.8	13.2 ± 1.3	15.5 ± 2.0	13.6 ± 2.7	8.9 ± 2.9	11.7 ± 2.0	7.9 ± 3.1*
	Uncalcified	20.7 ± 7.4	19.4 ± 0.7	21.5 ± 1.5	21.1 ± 3.1	12.7 ± 5.3	17.8 ± 4.4	11.6 ± 5.4
	Calcified	4.9 ± 0.9	3.7 ± 2.1	7.5 ± 3.3	5.3 ± 3.9	2.6 ± 1.7	2.9 ± 1.7	3.8 ± 1.3
TP	Total	13.3 ± 4.3	15.2 ± 3.3	13.6 ± 0.8	14.1 ± 0.3	10.0 ± 4.5	13.3 ± 3.6	10.1 ± 3.6
	Uncalcified	29.6 ± 13.0	35.6 ± 7.8	35.1 ± 5.4	34.5 ± 2.8	18.8 ± 9.2	26.5 ± 6.4	16.1 ± 5.0
	Calcified	5.5 ± 0.9	5.4 ± 2.1	4.1 ± 1.0	4.5 ± 1.1	4.7 ± 0.8	5.1 ± 2.1	5.8 ± 2.1

713 * Significant differences from the control group.

† Significant differences from the 2 weeks after the same intervention.

‡ Significant differences from the 4 weeks after the same intervention.

Supplementary Table 3. Staining intensity for type II collagen at each region after hindlimb unloading or joint immobilization.

		Control	Hindlimb Unloading			Joint Immobilization		
Region	Layer		2w	4w	8w	2w	4w	8w
FA	Total	135.7 ± 9.9	140.1 ± 5.2	131.2 ± 7.0	134.2 ± 7.0	132.2 ± 7.6	134.7 ± 5.1	140.3 ± 5.6
	Uncalcified	143.1 ± 13.8	152.9 ± 8.9	146.8 ± 4.5	142.8 ± 6.2	143.9 ± 9.6	146.9 ± 7.3	150.1 ± 5.0
	Calcified	133.5 ± 9.1	136.1 ± 4.5	126.7 ± 7.8	130.5 ± 8.2	128.9 ± 8.6	129.6 ± 8.2	135.7 ± 7.8
FM	Total	124.4 ± 12.6	126.5 ± 1.7	115.9 ± 3.9	117.9 ± 3.2	121.6 ± 13.3	120.2 ± 10.2	132.0 ± 6.2
	Uncalcified	125.6 ± 14.2	124.9 ± 4.9	115.3 ± 4.7	112.2 ± 6.9	120.7 ± 16.3	120.7 ± 6.3	136.9 ± 10.7
	Calcified	124.2 ± 13.5	127.3 ± 3.0	116.2 ± 3.8	120.3 ± 1.2	123.8 ± 13.7	120.7 ± 12.0	131.2 ± 7.1
FP	Total	125.3 ± 13.8	134.6 ± 1.7	119.8 ± 6.1	116.6 ± 7.2	129.9 ± 10.9	120.4 ± 13.4	141.8 ± 10.9
	Uncalcified	124.4 ± 17.5	122.0 ± 3.2	104.1 ± 4.1	102.1 ± 4.5*	120.9 ± 10.1	114.1 ± 9.0	136.3 ± 12.2
	Calcified	126.9 ± 12.9	140.1 ± 4.4	126.6 ± 6.9	124.4 ± 11.3	138.1 ± 13.1	127.1 ± 16.5	148.0 ± 12.1
TA	Total	115.4 ± 13.6	111.9 ± 6.4	122.0 ± 5.6	132.4 ± 6.1	120.6 ± 5.9	122.8 ± 7.5	110.7 ± 7.7
	Uncalcified	106.9 ± 16.7	104.3 ± 8.3	112.3 ± 2.0	122.0 ± 7.6	112.5 ± 6.3	113.4 ± 9.0	106.8 ± 8.8
	Calcified	123.4 ± 11.7	114.2 ± 6.2	124.1 ± 8.5	137.1 ± 4.9†	121.3 ± 9.4	130.3 ± 6.5	112.8 ± 7.5
TM	Total	129.6 ± 14.4	127.4 ± 5.5	123.5 ± 4.6	113.5 ± 2.1	126.5 ± 8.0	125.6 ± 7.4	137.7 ± 9.4
	Uncalcified	133.9 ± 19.0	130.8 ± 7.4	125.6 ± 4.1	115.6 ± 5.7	130.7 ± 8.9	129.5 ± 4.7	140.4 ± 7.2
	Calcified	126.1 ± 10.3	124.3 ± 6.3	120.8 ± 4.7	111.6 ± 2.2	118.9 ± 9.3	121.1 ± 10.7	134.5 ± 14.3
TP	Total	126.7 ± 14.4	123.7 ± 2.4	119.6 ± 5.8	117.5 ± 4.6	127.2 ± 13.2	127.4 ± 10.4	136.8 ± 10.2
	Uncalcified	137.6 ± 18.4	130.2 ± 0.7	126.0 ± 5.7	125.0 ± 9.7	138.1 ± 12.9	139.8 ± 2.7	144.2 ± 12.0
	Calcified	122.0 ± 13.2	122.4 ± 1.1	116.7 ± 6.2	113.3 ± 3.9	123.3 ± 13.6	126.2 ± 16.2	132.4 ± 13.5

* Significant differences from the control group.

† Significant differences from the 2 weeks after the same intervention.

Supplementary Table 4. Number of MMP13-positive cells (/10^4 μm^2) at each region after hindlimb unloading or joint immobilization.

		Control	Hindlimb Unloading			Joint Immobilization		
Region	Layer		2w	4w	8w	2w	4w	8w
FA	Total	3.6 ± 1.4	3.3 ± 1.0	4.8 ± 0.7	2.8 ± 1.1	2.5 ± 1.0	2.9 ± 0.6	1.8 ± 0.8
	Calcified	5.0 ± 2.0	4.4 ± 1.2	6.5 ± 1.1	3.9 ± 1.3	3.3 ± 1.5	4.1 ± 0.3	2.4 ± 1.0
FM	Total	1.6 ± 1.3	3.0 ± 1.0	4.1 ± 1.9	4.2 ± 0.8*	1.9 ± 1.0	3.5 ± 0.9	1.9 ± 1.0
	Calcified	2.6 ± 2.1	4.2 ± 1.1	5.5 ± 2.5	6.2 ± 0.9*	3.0 ± 1.7	5.1 ± 1.4	3.2 ± 1.5
FP	Total	3.6 ± 1.0	3.6 ± 1.1	3.9 ± 0.9	4.1 ± 2.3	3.2 ± 2.3	4.5 ± 1.3	2.7 ± 0.6
	Calcified	5.3 ± 1.7	5.1 ± 1.7	6.0 ± 1.6	6.0 ± 3.1	5.4 ± 3.7	7.2 ± 1.8	4.2 ± 0.7
TA	Total	2.5 ± 1.2	2.0 ± 1.0	3.2 ± 1.6	3.2 ± 0.6	2.6 ± 0.9	1.9 ± 0.8	1.5 ± 0.8
	Calcified	5.3 ± 2.6	3.1 ± 1.4	5.1 ± 2.5	5.6 ± 0.8	4.9 ± 1.4	3.4 ± 0.9	2.4 ± 1.5
TM	Total	2.9 ± 0.8	4.0 ± 2.6	4.3 ± 1.1	5.5 ± 3.2	1.9 ± 0.6	2.5 ± 1.1	2.9 ± 1.2
	Calcified	8.9 ± 3.4	11.6 ± 8.5	10.7 ± 1.8	12.5 ± 7.1	5.6 ± 1.5	6.3 ± 2.7	7.6 ± 3.8
TP	Total	4.8 ± 2.5	3.0 ± 1.0	4.1 ± 1.5	4.0 ± 3.1	3.1 ± 0.8	4.7 ± 2.6	4.4 ± 2.1
	Calcified	7.6 ± 3.8	4.3 ± 1.0	5.6 ± 2.2	5.7 ± 4.2	4.6 ± 1.0	7.6 ± 4.5	7.1 ± 2.9

* Significant differences from the control group.

Supplementary Table 5. Staining intensity for aggrecan at each region after hindlimb unloading or joint immobilization.

		Control	Hindlimb Unloading			Joint Immobilization		
Region	Layer		2w	4w	8w	2w	4w	8w
FA	Total	102.7 ± 4.3	95.7 ± 4.4	106.3 ± 4.1†	109.3 ± 4.5†	91.5 ± 4.5*	97.0 ± 3.7	95.7 ± 5.9
	Uncalcified	104.2 ± 6.4	91.1 ± 6.6*	102.5 ± 5.9	103.4 ± 5.1	84.3 ± 2.8*	94.8 ± 4.7	93.7 ± 6.9
	Calcified	102.1 ± 3.5	97.8 ± 5.4	106.4 ± 5.0	108.4 ± 6.1	93.2 ± 5.4*	96.9 ± 3.9	94.9 ± 5.9
FM	Total	96.8 ± 3.2	91.5 ± 3.1	98.4 ± 4.6	101.8 ± 2.1†	86.1 ± 2.3*	92.0 ± 0.3	95.5 ± 5.8†
	Uncalcified	94.9 ± 3.6	82.7 ± 3.5*	88.8 ± 5.4	92.2 ± 2.5†	77.8 ± 3.9*	88.3 ± 1.6†	96.4 ± 8.7†
	Calcified	98.9 ± 3.2	94.4 ± 3.2	101.3 ± 5.1	105.6 ± 2.2*†	90.6 ± 2.7*	94.7 ± 2.2	95.1 ± 5.3
FP	Total	94.8 ± 4.2	94.7 ± 4.0	100.3 ± 0.5	101.3 ± 1.8*	93.0 ± 2.9	103.0 ± 3.2*†	100.9 ± 3.6†
	Uncalcified	89.5 ± 4.0	80.5 ± 4.0*†	84.1 ± 3.6	81.8 ± 5.4	85.9 ± 6.0	109.1 ± 9.6*†	103.7 ± 10.3*†
	Calcified	99.5 ± 4.2	98.9 ± 5.0	104.7 ± 1.1	106.5 ± 2.3*†	98.4 ± 1.5	100.2 ± 2.9	100.1 ± 4.3
TA	Total	99.9 ± 6.2	100.0 ± 5.7	101.5 ± 6.3	100.3 ± 5.2	87.1 ± 4.4*	93.6 ± 2.1	94.1 ± 5.1
	Uncalcified	104.4 ± 7.0	97.9 ± 10.8	103.6 ± 5.8	101.3 ± 2.8	82.4 ± 5.9*	96.7 ± 2.7†	102.7 ± 4.6†
	Calcified	98.3 ± 8.5	100.3 ± 5.9	102.1 ± 8.3	100.3 ± 5.9	88.4 ± 4.0	92.9 ± 4.2	91.3 ± 4.6
TM	Total	100.2 ± 5.6	93.4 ± 4.8	97.8 ± 5.0	102.1 ± 4.0	91.3 ± 3.6*	96.6 ± 2.4	94.5 ± 1.4
	Uncalcified	103.6 ± 6.8	92.8 ± 8.7	98.2 ± 6.9	104.1 ± 2.2	90.6 ± 5.7*	100.0 ± 3.5	94.8 ± 2.5
	Calcified	100.1 ± 4.4	96.7 ± 3.2	98.8 ± 6.6	102.4 ± 6.4	95.4 ± 4.5	95.8 ± 4.4	95.6 ± 2.4
TP	Total	101.2 ± 9.8	93.3 ± 2.6*	99.4 ± 1.6	97.1 ± 5.0	96.7 ± 5.4	106.9 ± 7.1	104.2 ± 9.7
	Uncalcified	109.0 ± 14.0	86.6 ± 1.5	92.8 ± 6.2	98.3 ± 6.9	96.5 ± 11.8	120.5 ± 10.4	109.2 ± 13.9
	Calcified	100.1 ± 7.7	93.1 ± 1.9	100.1 ± 3.7	96.2 ± 4.7	96.8 ± 5.7	107.3 ± 6.7	104.4 ± 9.4

* Significant differences from the control group.

† Significant differences from the 2 weeks after the same intervention.

Supplementary Table 6. Number of ADAMTS5-positive cells (/10^4 μm^2) at each region after hindlimb unloading or joint immobilization.

		Control	Hindlimb Unloading			Joint Immobilization		
Region	Layer		2w	4w	8w	2w	4w	8w
FA	Total	16.2 ± 4.0	13.9 ± 1.1	15.9 ± 1.6	18.5 ± 5.0	19.9 ± 1.7	22.4 ± 3.4	17.1 ± 7.4
	Uncalcified	31.4 ± 5.0	33.8 ± 6.5	41.1 ± 1.9	39.0 ± 7.2	57.8 ± 4.3*	52.6 ± 12.9	38.7 ± 23
	Calcified	9.7 ± 2.6	7.8 ± 1.6	7.0 ± 2.2	8.8 ± 3.9	6.0 ± 1.9	10.3 ± 3.2	9.8 ± 6.1
FM	Total	15.5 ± 2.3	16.2 ± 4.6	14.4 ± 2.3	15.6 ± 3.0	19.2 ± 3.8	19.7 ± 3.3	18.5 ± 4.9
	Uncalcified	26.9 ± 4.5	35.6 ± 13.5	32.2 ± 5.4	31.6 ± 9.1	43.8 ± 13.8*	36.7 ± 4.8	34.3 ± 6.0
	Calcified	8.8 ± 2.1	8.1 ± 2.0	7.3 ± 1.6	7.5 ± 1.4	7.8 ± 2.0	8.9 ± 2.1	7.7 ± 4.2
FP	Total	5.9 ± 2.4	21.0 ± 7.2*	18.6 ± 4.4*	20.8 ± 4.1*	12.0 ± 7.0	6.9 ± 2.3	8.1 ± 4.3
	Uncalcified	10.3 ± 5.0	40.6 ± 8.0*	34.3 ± 6.1*	43.8 ± 7.4*	20.8 ± 10.4	11.8 ± 7.6	12.1 ± 13.6
	Calcified	3.4 ± 1.6	9.3 ± 6.1	8.2 ± 3.7	8.9 ± 2.6	5.2 ± 2.6	4.1 ± 1.5	4.7 ± 3.4
TA	Total	16.1 ± 4.8	12.6 ± 2.5	16.7 ± 2.4	14.6 ± 1.9	17.8 ± 2.9	22.7 ± 5.4	18.7 ± 3.8
	Uncalcified	23.6 ± 7.1	23.4 ± 7.0	31.8 ± 4.7	26.1 ± 5.3	31.1 ± 3.9	39.3 ± 12.3	45.9 ± 17.4*
	Calcified	5.4 ± 3.7	6.0 ± 1.3	5.6 ± 2.6	8.3 ± 3.1	5.1 ± 4.9	7.8 ± 1.3	6.8 ± 1.3
TM	Total	13.7 ± 2.0	13.2 ± 0.5	18.6 ± 2.8*†	16.3 ± 2.3	19.4 ± 3.6*	14.6 ± 3.8	14.7 ± 1.9
	Uncalcified	17.1 ± 1.5	18.3 ± 2.3	26.2 ± 5.3*†	24.2 ± 3.4*	23.2 ± 3.6*	16.7 ± 2.9	21.4 ± 4.7
	Calcified	7.2 ± 3.7	5.1 ± 1.2	7.2 ± 3.2	5.5 ± 2.4	12.5 ± 4.8	11.3 ± 7.8	5.8 ± 2.2
TP	Total	11.5 ± 2.6	17.9 ± 4.4	13.9 ± 3.5	20.4 ± 8.7	14.6 ± 5.3	11.6 ± 4.9	8.1 ± 4.1
	Uncalcified	19.3 ± 5.2	44.0 ± 13.7*	33.4 ± 11.8	47.9 ± 22.9	25.7 ± 9.5	16.3 ± 12.5	10.2 ± 10.6
	Calcified	5.9 ± 1.8	4.8 ± 1.7	5.1 ± 1.0	6.1 ± 2.2	7.5 ± 3.9	8.1 ± 2.6	6.5 ± 1.2

* Significant differences from the control group.

† Significant differences from the 2 weeks after the same intervention.

Supplementary Table 7. Number of ALP-positive cells (/10^4 μm^2) at each region after hindlimb unloading or joint immobilization.

		Control	Hindlimb Unloading			Joint Immobilization		
Region	Layer		2w	4w	8w	2w	4w	8w
FA	Total	21.2 ± 3.2	21.2 ± 2.7	21.1 ± 3.9	19.4 ± 1.6	20.5 ± 1.2	22.1 ± 5.0	23.3 ± 4.7
	Uncalcified	38.6 ± 11.6	37.3 ± 6.4	35.6 ± 6.2	41.1 ± 5.6	44.5 ± 4.4	47.7 ± 7.6	75.4 ± 16.6*†‡
	Calcified	15.6 ± 2.0	15.1 ± 3.9	14.4 ± 3.4	7.5 ± 3.3*†‡	12.9 ± 2.0	12.2 ± 4.7	10.8 ± 4.2
FM	Total	20.2 ± 4.2	18.4 ± 1.4	17.3 ± 2.8	15.6 ± 3.8	17.6 ± 3.6	20.9 ± 3.4	18.2 ± 2.0*
	Uncalcified	24.9 ± 4.3	28.6 ± 3.0	34.1 ± 7.1*	33.2 ± 3.9	29.2 ± 7.5	36.8 ± 7.5	38.6 ± 8.2
	Calcified	17.7 ± 4.4	14.0 ± 2.5	11.5 ± 2.1	7.0 ± 5.0*	11.9 ± 3.4	12.5 ± 3.1	7.5 ± 1.5*
FP	Total	19.1 ± 2.8	16.0 ± 2.5	18.0 ± 2.5	15.9 ± 1.6	14.9 ± 2.5	12.2 ± 2.5*	10.0 ± 5.0*
	Uncalcified	20.6 ± 5.5	30.3 ± 7.4	30.6 ± 4.0	30.1 ± 5.7	18.5 ± 3.8	18.5 ± 6.0	18.9 ± 8.9
	Calcified	18.3 ± 1.7	10.7 ± 1.9*	11.7 ± 2.3*	8.9 ± 3.1*	12.2 ± 2.4*	7.9 ± 1.9*	4.9 ± 2.6*†
TA	Total	14.8 ± 2.6	17.8 ± 2.6	15.8 ± 1.1	17.9 ± 7.8	16.3 ± 1.0	21.8 ± 3.8*	20.4 ± 2.4*
	Uncalcified	14.0 ± 1.7	27.2 ± 7.6	22.5 ± 2.4	37.1 ± 18.9*	23.2 ± 2.9	37.4 ± 13.7*†	38.2 ± 3.7*†
	Calcified	16.2 ± 5.7	11.9 ± 2.3	10.9 ± 2.0	7.5 ± 2.9*	10.5 ± 2.6	12.7 ± 1.7	11.6 ± 2.6
TM	Total	10.7 ± 1.6	12.4 ± 1.8	13.5 ± 1.8	10.8 ± 1.7	10.5 ± 2.6	11.6 ± 1.3	11.4 ± 1.1
	Uncalcified	7.1 ± 1.4	11.4 ± 1.2*	12.7 ± 1.6*	11.9 ± 1.2*	9.9 ± 2.5	11.1 ± 3.4	13.0 ± 5.0*
	Calcified	17.4 ± 3.0	14.0 ± 3.6	14.5 ± 3.8	9.3 ± 4.6*	11.8 ± 3.3	13.0 ± 3.6	10.2 ± 2.9*
TP	Total	17.5 ± 1.9	18.9 ± 2.5	18.8 ± 2.6	14.5 ± 0.7*†	13.0 ± 2.8*	7.4 ± 2.5*†	6.1 ± 0.9*†
	Uncalcified	19.6 ± 6.2	26.1 ± 1.7	29.6 ± 9.5	26.0 ± 4.5	16.3 ± 3.7	7.0 ± 2.8*	8.7 ± 2.9*
	Calcified	15.3 ± 2.6	14.2 ± 3.2	13.5 ± 1.6	6.6 ± 2.9*†‡	11.0 ± 3.6	7.7 ± 2.6*	4.2 ± 1.5*†

* Significant differences from the control group.

† Significant differences from the 2 weeks after the same intervention.

‡ Significant differences from the 4 weeks after the same intervention.

Supplementary Table 8. Number of type X collagen-positive cells (/10^4 μm^2) at each region after hindlimb unloading or joint immobilization.

		Control	Hindlimb Unloading			Joint Immobilization		
Region	Layer		2w	4w	8w	2w	4w	8w
FA	Total	10.4 ± 1.1	9.9 ± 1.5	9.7 ± 1.4	9.1 ± 1.7	9.5 ± 3.9	9.1 ± 0.4	12.5 ± 1.1
	Calcified	13.3 ± 0.5	12.2 ± 1.6	12.9 ± 1.9	12.4 ± 2.4	12.3 ± 4.7	12.6 ± 1.7	14.5 ± 0.9
FM	Total	7.3 ± 0.3	6.3 ± 1.3	8.6 ± 4.0	8.6 ± 0.5	8.0 ± 1.3	9.3 ± 1.7	6.1 ± 0.4
	Calcified	10.2 ± 0.4	8.9 ± 0.4	11.9 ± 5.6	11.9 ± 2.1	11.1 ± 1.0	14.9 ± 0.7*†	8.9 ± 0.5‡
FP	Total	10.0 ± 4.2	7.1 ± 2.0	6.6 ± 2.1	8.1 ± 2.0	9.3 ± 1.4	8.4 ± 1.9	7.5 ± 1.7
	Calcified	14.9 ± 6.7	9.4 ± 2.9	8.5 ± 2.4	10.9 ± 1.5	13.9 ± 1.3	13.2 ± 3.5	12.7 ± 5.1
TA	Total	6.9 ± 1.2	7.4 ± 2.5	7.4 ± 1.0	4.6 ± 1.5	6.9 ± 4.1	4.7 ± 0.9	4.2 ± 0.7
	Calcified	12.4 ± 0.4	11.4 ± 5.2	11.3 ± 2.8	7.3 ± 1.7	11.1 ± 7.3	9.3 ± 0.4	6.8 ± 1.9
TM	Total	3.8 ± 1.6	5.0 ± 1.0	4.3 ± 0.4	3.6 ± 0.6	5.5 ± 3.1	4.5 ± 0.9	4.9 ± 0.3
	Calcified	9.2 ± 4.2	10.0 ± 1.4	10.2 ± 0.8	7.7 ± 0.3	11.1 ± 6.6	10.5 ± 0.0	9.0 ± 1.7
TP	Total	9.6 ± 1.3	7.7 ± 0.3	5.2 ± 1.6	6.4 ± 1.9	8.0 ± 1.1	7.7 ± 2.9	7.1 ± 0.3
	Calcified	13.8 ± 0.2	9.6 ± 0.2	7.3 ± 1.2*	8.8 ± 2.0*	12.6 ± 0.9	12.3 ± 5.7	10.7 ± 0.6

* Significant differences from the control group.

† Significant differences from the 2 weeks after the same intervention.

‡ Significant differences from the 4 weeks after the same intervention.

Supplementary Table 9. Number of VEGF-positive cells (/10^4 μm^2) at each region after hindlimb unloading or joint immobilization.

		Control	Hindlimb Unloading			Joint Immobilization		
Region	Layer		2w	4w	8w	2w	4w	8w
FA	Total	16.8 ± 0.4	12.1 ± 2.0	12.5 ± 1.0	10.1 ± 3.7	8.6 ± 2.3	6.3 ± 1.7	8.4 ± 5.2
	Uncalcified	30.6 ± 9.5	19.7 ± 1.7	24.0 ± 0.5	15.5 ± 10.9	22.9 ± 7.0	13.3 ± 2.6	14.0 ± 19.8
	Calcified	12.0 ± 2.4	10.0 ± 2.2	8.7 ± 1.6	7.9 ± 0.7	4.8 ± 2.3	4.5 ± 1.2	6.3 ± 1.6
FM	Total	12.0 ± 2.3	7.9 ± 0.8	11.7 ± 1.1	10.1 ± 0.7	6.1 ± 1.1	7.7 ± 1.3	13.6 ± 2.1†
	Uncalcified	18.9 ± 0.5	10.1 ± 2.0	19.3 ± 7.1	17.0 ± 2.4	12.8 ± 0.1	16.4 ± 3.3	25.4 ± 3.2†
	Calcified	8.4 ± 3.3	7.2 ± 1.5	8.7 ± 1.5	7.6 ± 0.4	3.2 ± 0.8	3.0 ± 1.4	6.4 ± 5.1
FP	Total	15.5 ± 1.4	11.2 ± 0.2	8.0 ± 0.5*	9.4 ± 1.9*	11.7 ± 3.1	9.4 ± 0.2	6.9 ± 1.7*
	Uncalcified	25.4 ± 1.1	15.5 ± 4.3	9.4 ± 0.0	17.0 ± 6.9	17.8 ± 5.1	11.9 ± 8.0	2.7 ± 1.1*
	Calcified	9.1 ± 1.3	9.4 ± 1.4	7.3 ± 0.8	6.2 ± 0.4	8.0 ± 2.3	8.0 ± 4.1	8.8 ± 2.5
TA	Total	15.1 ± 1.4	11.2 ± 1.2	15.3 ± 5.2	7.8 ± 0.8	7.7 ± 1.6	18.9 ± 1.3	8.1 ± 3.7
	Uncalcified	24.5 ± 1.8	19.5 ± 8.8	22.1 ± 7.6	9.8 ± 1.9	14.4 ± 2.4	31.9 ± 3.9†	19.2 ± 14.6‡
	Calcified	8.8 ± 0.6	7.4 ± 1.7	11.8 ± 4.6	6.4 ± 2.7	3.3 ± 1.3	6.9 ± 4.2	2.5 ± 1.1
TM	Total	14.7 ± 1.0	10.1 ± 1.3	13.5 ± 1.6	11.4 ± 4.5	12.9 ± 2.4	11.7 ± 1.4	9.6 ± 3.4
	Uncalcified	16.9 ± 1.7	12.7 ± 0.5	17.1 ± 4.3	14.1 ± 8.3	19.1 ± 2.6	13.3 ± 1.2	14.6 ± 5.3
	Calcified	10.9 ± 0.2	5.9 ± 4.2	6.6 ± 3.8	8.3 ± 0.2	4.3 ± 0.1	8.6 ± 6.2	4.0 ± 1.3
TP	Total	16.5 ± 1.7	10.3 ± 1.3	12.6 ± 2.7	10.3 ± 0.6	13.5 ± 1.5	10.6 ± 0.8	7.1 ± 1.8*†
	Uncalcified	25.9 ± 1.2	14.1 ± 0.9*	22.2 ± 2.1†	19.6 ± 2.2	22.7 ± 5.3	21.8 ± 0.4	2.2 ± 3.2*†‡
	Calcified	7.0 ± 1.1	8.6 ± 2.1	8.3 ± 1.8	7.0 ± 0.1	8.8 ± 0.4	5.5 ± 1.8	10.8 ± 0.4‡

* Significant differences from the control group.

† Significant differences from the 2 weeks after the same intervention.

‡ Significant differences from the 4 weeks after the same intervention.